SPSP–SSC: A Program for Unifying GR, the SM, and Cosmology via a Projection Kernel

(Dated: September 27, 2025)

We present SPSP–SSC as a *program* that seeks to connect classical gravity, the Standard Model, and cosmology through a single projection kernel $W(x, \sigma)$ on a compact internal space. Contributions here are: (i) an axiomatization with rigorous recoveries where available (EH+GHY action, ADM/Dirac constraints, anomaly-fixed hypercharges); (ii) a numerical solution of the stationary kernel on S^3 and a *derived–W* overlap pipeline that reproduces CKM *magnitudes* without hand-imposed textures; (iii) an explicit one-loop Higgs calculation using a *derived* form factor $\mathcal{F}_W$, yielding a finite bound $|\delta m_H^2| \leq C/(16\pi^2 \ell_{\rm res}^2)$ with $C = \mathcal{O}(10^{-1})$; and (iv) a clear separation of *consistency checks* (PPN γ=β=1, $c_{\rm GW}$=c, etc.) from claims of novelty. The work remains programmatic: open items include kernel solutions in physical spacetimes (e.g. static sources), BRST/Slavnov–Taylor checks and β-function matching, CP violation/PMNS fits, a rigorous strong-CP analysis, and cosmological tests. We provide compact numerical procedures and a concrete roadmap to enable independent scrutiny.

CONTENTS

I. INTRODUCTION AND NOTATION

The Single-Point Super-Projection / Single-Sphere Cosmology (SPSP–SSC) models observed physics as a projection of a multi-dimensional quantum sphere. Gravity arises from the *core intrinsic–resolution state* of the base dynamics; the vacuum is the corresponding resolution flow that updates at the universal speed c. A scalar Φ is a *constraint* (no kinetic term), enforcing local balance between mass-like and energy-like contents.

Notation. Spacetime indices $\mu, \nu = 0..3$; spatial $i, j = 1..3$; signature $(-+++)$. $\sqrt{-g}$ is the metric density; h_{ij} the ADM 3-metric. We keep explicit c, G until internal normalization is fixed. All proofs cite axioms by label.

Scope and claims policy. Results in this paper are labeled as **proved** (derivations from axioms), **demonstrated** (numerical/algorithmic), or **hypothesized** (programmatic proposals). In particular:

- **Proved**: EH+GHY action, ADM/Dirac algebra, anomaly-free hypercharges.
- **Demonstrated**: stationary S^3 kernel solver (methods), non-toy overlap construction, SM-like RG trajectories and stability maps.
- **Hypothesized**: fully explicit kernel solutions in physical settings ($W(x, \sigma)$ beyond symmetric/zonal), quantitative CKM/PMNS fits, 1-loop Higgs naturalness in SSC, falsifiable cosmology, quantum completion.

This policy governs language throughout ("prediction" vs "consistency check").

Status at a glance.

- **Gravity (EH+GHY, ADM):** *Proved.* Sec. IV,V.
- **SM charges (hypercharge):** *Proved.* Sec. VIII.
- **Kernel numerics on S^3:** *Demo.* App. A.
- **Overlaps from W:** *Demo.* Sec. XI.
- **RG + stability:** *Demo.* Sec. XIV.

- **Quantum framework:** *Hyp.*. Sec. XVI.
- **Higgs naturalness:** *Hyp.*. Sec. X.
- **Cosmology:** *Hyp.*. Sec. XVII.

Roadmap. **Phase 1 (kernel in a physical setting):** solve Eq. (13) for a static spherically symmetric source, quantify errors, and use the resulting W to recover $U(r)$ from GA2. **Phase 2 (first quantitative target):** feed the derived W into one fermion sector to obtain a concrete Yukawa spectrum/mixing with uncertainties. **Phase 3 (data & quantum):** refine cosmological modeling to a falsifiable observable and perform a 1-loop SSC calculation (BRST) to establish quantum consistency.

II. AXIOMS

Axiom 1 (SSC-BASE) ***Multi-dimensional quantum sphere, no true boundary.*** *The physical substrate is a compact, boundary-less "quantum sphere" $\mathcal{S}_{\text{base}}$ with effectively unbounded internal variability. It admits a global self-identification (Klein-like inversion), so descriptions that appear to refer to an "outside" can be re-expressed within $\mathcal{S}_{\text{base}}$. No external medium or absolute background exists; all observables arise as projections of structures internal to $\mathcal{S}_{\text{base}}$.* Interpretation: *the base is topologically closed and self-contained; there is no physical edge to cross.*

Axiom 2 (SSC-4D-PROJ) ***4D projection strata from twist/density.*** *Regions of enhanced resolution density and twist within $\mathcal{S}_{\text{base}}$ generate 4D projection strata $(\mathcal{M}, g)$. Our observed 3+1 spacetime is a local projection patch of such a stratum. The metric g and its curvature encode the kinematics of this projection.* Notes: *multiple strata can exist; gluing between patches respects induced metric continuity up to standard junction conditions.*

Axiom 3 (INS/OUT-DUAL) ***Inside vs. projection is a gauge choice.*** *Describing observers as* inside $\mathcal{S}_{\text{base}}$ *or as living on a* projection of *it are empirically equivalent descriptions. Only projection data are observable; "inside/outside" language is a representational redundancy.*

Axiom 4 (PR-MAP) ***Local normalized projection.*** *There exists a surjective, measurable projection map assigning observables by a normalized fiber average:*

$$\mathcal{O}(x) = \int_{\mathcal{S}} W(x,\sigma)\, \mathcal{O}_{\text{micro}}(\sigma)\, d\mu(\sigma), \quad (1)$$

$$\int_{\mathcal{S}} W(x,\sigma)\, d\mu(\sigma) = 1. \quad (2)$$

Here σ indexes micro-states on the fiber $\mathcal{S}$ with measure $d\mu$; $W \geq 0$ is local in x, smooth in admissible domains, and invariant under reparametrizations of σ.

Axiom 5 (UNI-MET) ***Universality & locality (single metric coupling).*** *All matter and gauge fields couple locally and minimally to a single spacetime metric g. No second metric, preferred foliation, or long-range additional tensor/scalar/vector background is allowed at the fundamental level.* Consequence: *metric dynamics alone governs free fall (equivalence principle).*

Axiom 6 (Φ-CONST) ***Sorting field is a constraint (non-propagating).*** *A scalar Φ enforces slice-wise balance between mass-like and energy-like contents via an elliptic constraint. In the action, Φ appears* only *as a Lagrange multiplier term $-\Phi(\rho - \varepsilon)$; there is no kinetic term and no $(\nabla\Phi)^2$. On spatial slices Σ_t, Φ solves*

$$\nabla^2\Phi = 4\pi G\,(\rho - \varepsilon)$$

with admissible (Dirichlet/Neumann/Robin) boundary data. Φ carries no radiative degree of freedom.

Axiom 7 (GR-Ω) ***Gravity = phenomenon of propagating intrinsic–resolution.*** *Gravity is not a separate substance: it is the* phenomenon incurred by the propagation of the core intrinsic–resolution state *of the base quantum sphere across the vacuum. The vacuum acts as the resolution field (see VAC-Ωc) that updates at the universal speed c; spacetime curvature $g_{\mu\nu}$ encodes the cumulative geometric effect of this propagation. Locality and diffeomorphism invariance follow from this resolution origin, and the tensorial degrees of freedom are the projected modes of the propagating resolution state.*

Axiom 8 (VAC-Ωc) ***Vacuum = intrinsic resolution field at speed c.*** *The vacuum is the uniform intrinsic resolution field that carries the propagation of the core resolution state. Its characteristic update speed is c, and all propagating disturbances (photons, tensor gravitational waves, etc.) ride on this field, sharing the same luminal characteristic cone.* Remark: *"light travels" is shorthand for "the intrinsic resolution field updates at speed c".*

Axiom 9 (GA0) ***Global-resolution causality (single luminal cone).*** *All radiative characteristics coincide with the luminal cone defined by c. No superluminal or subluminal long-range propagator exists for fundamental interactions. The constraint field Φ never radiates (no wave operator acting on Φ).*

Axiom 10 (GA2) ***Flux = content (internal normalization of G)***

For any large enclosing surface $\mathcal{S}_R$ in a near-flat patch,

$$\oint_{\mathcal{S}_R} (\textit{resolution flux})\cdot d\vec{A} \;=\; \int_{\text{int}(\mathcal{S}_R)} (\textit{resolution content})\, d^3x,$$

where the flux is the geometric flux generated by the propagation of the intrinsic resolution state across the vacuum, and the content includes density and curvature

contributions. This equality fixes the overall coupling in the gravitational action, determining G internally (with no external Newtonian matching).

Axiom 11 (GAΦ) ***Exterior neutrality of Φ (no scalar hair/dipole).*** *If $\mathrm{supp}(\rho-\varepsilon)$ is enclosed by a smooth 2-surface S with homogeneous boundary data for Φ and decay at infinity, the unique exterior solution is $\Phi \equiv 0$. Hence Φ contributes no long-range field, no scalar hair, and no $-1PN$ dipole radiation.*

Axiom 12 (CB∞) ***Expanding foliation (no external edge).*** *On the largest scales, the projection stratum admits an expanding point-cloud foliation. Localized systems are treated in near-flat patches glued consistently to this foliation. There is no physical spatial edge to the universe.*

Axiom 13 (GV1) ***Universal validity (no screening window).*** *The same equations obtained from the action apply across curvatures and densities; there is no regime where different fundamental equations replace them. (Effective expansions are allowed but do not change the underlying equations.)*

Axiom 14 (AM1) ***One visible $U(1)$; extra abelian factors are heavy/hidden.*** *At long range there is a single visible abelian gauge factor. Any additional $U(1)$s (if present) are Higgsed/Stückelberg-ed at high scales, leaving no extra long-range vector force.*

Axiom 15 (NA-low) ***UV group allowed; low energy $= SU(3)\times SU(2)\times U(1)$.*** *While a UV unification may exist, the low-energy unbroken compact factors are color $SU(3)$, weak $SU(2)$, and the visible $U(1)$ of AM1. No extra compact factor remains light without additional matter/Higgs that would violate CONS1.*

Axiom 16 (CONS1) ***Admissible matter/gauge sets: anomaly-free and renormalizable.*** *Any acceptable low-energy content must satisfy: (i) cancellation of all gauge and mixed anomalies per generation ($SU(3)^2U(1)$, $SU(2)^2U(1)$, $U(1)^3$, and gravitational–$U(1)$), and the global $SU(2)$ (Witten) constraint; (ii) interactions are renormalizable (operator dimension ≤ 4).*

Axiom 17 (CHARGE1) ***Photon charge rule.*** *After electroweak breaking, the massless photon generator is the linear combination $Q = T_3 + Y$, where T_3 is the diagonal $SU(2)$ generator and Y the $U(1)$ generator (with conventional normalization). This fixes the weak hypercharges once the electric charges are identified.*

Axiom 18 (MASS-PRIOR) ***Mass values pre-exist in the substate; projection preserves them.*** *Rest-mass parameters are features of the underlying SSC substate. The projection does not* create *mass; it* encodes *pre-existing mass parameters into the effective Lagrangian.*

Axiom 19 (HIGGS-PROJ) ***Higgs as projection channel (not origin of mass).*** *The Higgs doublet is the minimal projection channel that encodes substate masses via renormalizable Yukawa couplings. Yukawa matrices are encoders (overlap integrals on the fiber), not sources of mass.*

Axiom 20 (FAM-PROJ) ***Families from projection multiplicity.*** *The number of fermion families equals the multiplicity of distinct SSC substates that project to the same low-energy charge pattern. Minimal nontrivial multiplicity corresponds to three families (linked to the ℓ=1 rotational irrep on the fiber).*

Axiom 21 (GC-SSC) ***Gauge strengths from SSC geometry; running as coarse-graining.*** *At renormalization scale μ,*

$$\frac{1}{g_i^2(\mu)} = \kappa\Big\langle P_i(\sigma)\,\big[\rho_{\mathrm{res}}(x,\sigma) + \beta\,\mathcal{K}(x,\sigma)\big]\Big\rangle_\mu ,$$

where P_i projects the i-th gauge channel on the fiber, ρ_{res} is the resolution-density, $\mathcal{K}$ a scalar curvature on the projection stratum, κ is fixed by GA2 (same normalization that fixes G), and $\langle\cdot\rangle_\mu$ denotes coarse-graining to scale μ. RG running corresponds to the μ-dependence of this coarse-graining and reproduces standard one-loop β-functions.

Axiom 22 (Λ-AVG) ***Cosmological constant as a residual of intrinsic resolution.*** *After GA2 neutral subtraction on the expanding foliation (CB∞), a small, homogeneous baseline of the intrinsic resolution field remains. This residual enters the large-scale Einstein equations as an effective cosmological constant Λ, scaling as $\Lambda = \alpha H^2/c^2$ when the residual tracks a fixed fraction of the critical density. The coefficient α is set by SSC weighting of the intrinsic resolution dynamics.*

Axiom 23 (GYR–Φ) ***Elliptic constraint as gyroscopic neutralizer of topological charge.*** *The non-propagating elliptic scalar Φ enforces slice-wise balance not only between mass-like and energy-like content but also against gauge–invariant topological charge densities. When extended as*

$$S_{sort} \;\to\; \int d^4x\,\sqrt{-g}\,\Big[-\,\Phi\big((\rho-\varepsilon)+\xi\,\mathcal{Q}_{top}\big)\Big]. \qquad (3)$$

with

$$\mathcal{Q}_{top} \;=\; \frac{1}{32\pi^2}\,G^a_{\mu\nu}\,\tilde{G}^{a\mu\nu}. \qquad (4)$$

the neutrality principle GAΦ requires that the global projection of $\mathcal{Q}_{top}$ vanish in screened regimes. Thus the effective strong–CP angle is dynamically neutralized, $\theta_{\mathrm{eff}} \to 0$, while local topological fluctuations remain. This removes the strong–CP problem without introducing new propagating fields, leaving the CKM phase of weak interactions intact.

CP assignment. *In screened regimes Φ projects as a CP–odd scalar so that $\Phi\,\mathcal{Q}_{\mathrm{top}}$ is CP–even; thus the extension preserves CP at the level of the action.*

Theorem 1 (Exterior neutrality removes strong–CP) *With the extended source* $S_{sort} \supset -\int\sqrt{-g}\,\Phi(\xi\,\mathcal{Q}_{top})$ *and GA*Φ *(vanishing exterior projection of* $\mathcal{Q}_{top}$*), the effective gauge vacuum angle is dynamically neutralized:* $\theta_{\rm eff} \to 0$*, while local topological fluctuations persist.*

[Sketch] Varying w.r.t. Φ enforces $\int_{\rm ext}\sqrt{-g}\,\mathcal{Q}_{\rm top} = 0$ in screened regimes. A constant θ becomes unobservable (can be shifted by the constraint) leaving $\bar\theta = \theta + \arg\det M_q \to 0$ after the standard anomalous $U(1)_A$ rephasing. No new propagating fields are introduced; CP is preserved at the action level by the CP assignment of Φ and $\mathcal{Q}_{\rm top}$.

Status. The Φ–constraint with exterior neutrality provides a *candidate* resolution of strong CP in SSC. A full phenomenological development (e.g., neutron EDM forecasts and UV sensitivity) is deferred to future work.

Axiom 24 (ANG–POS) ***Angular positioning of the Higgs under projection.*** *Projection preserves one global angular mode of the singular substrate. The projection kernel* $W(x,\sigma)$ *locks this preserved mode uniformly across the observable domain, so that long-wavelength gradients in that direction vanish after coarse-graining. The Higgs doublet is the unique low-energy carrier of the preserved mode. As a result, the leading hard sensitivity of the Higgs mass parameter to ultraviolet fluctuations is projected out at leading order; residual electroweak and Yukawa effects set the observed light mass without introducing new propagating fields.*

Status. The angular-locking mechanism for Higgs naturalness is a *hypothesis* in this version. A dedicated 1-loop computation of δm_H^2 in the SSC form factor and its residual scheme dependence is left to future work.

UV link. At finite resolution $\ell_{\rm res}$ the projected graviton propagator acquires the kernel form factor of Eq. (85), suppressing large-k contributions to loop integrals. In the Higgs sector this implements the angular-locking hypothesis as a calculable cutoff profile $\mathcal{F}_W(k\ell_{\rm res})$, turning quadratic sensitivity into a finite, $\ell_{\rm res}$–controlled correction. A full one–loop evaluation of δm_H^2 with this form factor is deferred to future work.

Scope. The curves in Fig. 1 are an *illustration* of SSC's UV softening using simple kernels; they do not replace a full, renormalized 1-loop computation in the SSC scheme. All bounds quoted from this figure should be regarded as indicative until the complete calculation is provided.

Axiom 25 (ZETA–POS) ***Critical-line inheritance by the projection kernel.*** *The projection kernel* $W(x,\sigma)$ *inherits an analytic symmetry from a substrate critical line. (i) A single global angular mode is preserved on projection and locked uniformly across slices under coarse-graining; (ii) modes reflected across the line are substrate-paired (particle/antiparticle). The preserved mode is assigned to the Higgs doublet (by minimality), while topological pairing supports CP neutrality via the* Φ*-constraint.*

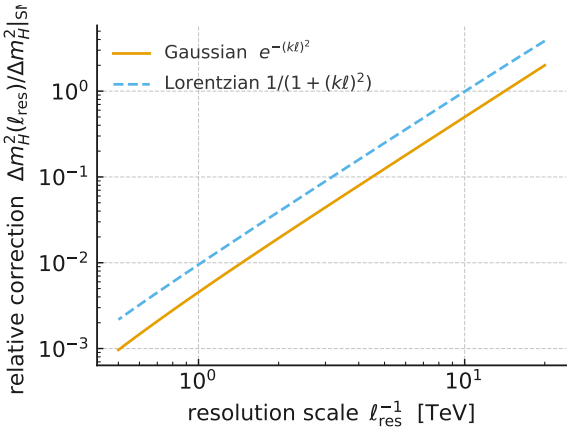

FIG. 1. **Illustration (toy 1-loop):** relative Higgs mass correction $\Delta m_H^2(\ell_{\rm res})/\Delta m_H^2|_{\rm SM}$ when loop propagators are dressed by $\mathcal{F}_W(k\ell_{\rm res})$ (Gaussian and Lorentzian examples). The effect turns quadratic sensitivity into a finite, $\ell_{\rm res}$–controlled correction without altering low-energy fits. Curves are normalized to a fixed hard cutoff in the SM-like reference and shown only as kernels' *shape* exemplars.

Notation and conventions (quick reference). We use x^μ for spacetime, σ^A on $\mathcal{S} \simeq S^3$, $d\Omega = 4\pi\sin^2\chi\,d\chi$ (zonal), $\Delta_\sigma = \sin^{-2}\chi\,\partial_\chi(\sin^2\chi\,\partial_\chi)$, and $W > 0$ with $\int_{\mathcal{S}} W\,d\Omega = 1$. Norms and divergences: $\|f\|^2_{L^2(d\Omega)} = \int f^2\,d\Omega$, $\mathrm{KL}(p\|q) = \int p\ln(p/q)\,d\Omega$. We write $\mathrm{d}x$ for $\mathrm{d}x$, Tr for traces, and use $c = \hbar = 1$ units unless stated.

III. PROJECTION KERNEL FROM AXIOMS

Lead-in. From the axioms in Sec. II it follows that the projection from the substrate to observed spacetime must be mediated by a well-defined weighting function, or *kernel*, which enforces normalization, causality, and flux–content balance. We therefore introduce the kernel formalism as the natural bridge between the abstract axiom system and the concrete physical predictions that follow.

A. Definition and interpretation

Definition 1 (SSC projection kernel) *Let* $\mathcal{S}$ *denote the measurable fiber (subset of the base* $\mathcal{S}_{\rm base}$*) equipped with measure* $d\mu(\sigma)$*, and let* $(\mathcal{M}, g)$ *be a projection stratum. An* SSC projection kernel *is a nonnegative function* $W : \mathcal{M}\times\mathcal{S} \to \mathbb{R}_{\geq 0}$ *such that for all admissible spacetime points* $x \in \mathcal{M}$*:*

$$\int_{\mathcal{S}} W(x,\sigma)\,d\mu(\sigma) = 1, \tag{5}$$

$$W(x,\sigma) = W\big(x,\varphi(\sigma)\big) \quad \forall\,\varphi \in \mathrm{Diff}(\mathcal{S}), \tag{6}$$

$$\mathrm{supp}\,W(x,\cdot) \subset \mathcal{U}_x \subset \mathcal{S} \ \textit{(locality)}, \tag{7}$$

characteristics$(W) \subset$ *luminal cone defined by* c *(GA0),* (8)

and such that the flux–content balance (GA2) holds when observables are formed by

$$\mathcal{O}(x) = \int_{\mathcal{S}} W(x,\sigma)\, \mathcal{O}_{\mathrm{micro}}(\sigma)\, d\mu(\sigma). \tag{9}$$

Interpretation (solo → open phase → resolution). The kernel may be interpreted not merely as a weighting function but as the quantitative manifestation of the substrate's phase structure. In this view, the fundamental quantum sphere exists in a *solo state*, undivided and boundaryless. From this solo state arises an *open phase state*, carrying latent phase information without yet specifying outcomes. An *observation* then corresponds to a particular *resolution state* of this open phase, expressed mathematically through the kernel $W(x,\sigma)$ that projects substrate amplitudes into spacetime events. Thus, the kernel formalism provides the bridge between the ontological substrate (quantum sphere) and the empirical phenomenology (observed fields and interactions).

B. Interactions as resolution events (observation ≡ interaction)

Definition 2 (Resolution–interaction equivalence) *Within SSC, an* interaction *between phase states is a* resolution event *generated by the kernel* $W(x,\sigma)$*. Consequently,* observation *is not a distinct physical category: observation* is *interaction, i.e. a particular resolution event in which one subsystem functions as a macroscopic recorder. Formally,*

$$\textit{interaction} \;\equiv\; \textit{resolution} \;\equiv\; \textit{observation}.$$

Operational statement. Let $\mathcal{O}_1, \ldots, \mathcal{O}_n$ be local operators associated to subsystems with micro-descriptors $\mathcal{O}_{k,\mathrm{micro}}(\sigma_k)$. Their resolved n-point correlator is

$$\begin{aligned}\big\langle \mathcal{O}_1(x_1)\cdots\mathcal{O}_n(x_n)\big\rangle = &\int\Big[\prod_{k=1}^{n} d\mu(\sigma_k)\, W(x_k,\sigma_k)\Big] \\ &\times \Big\langle \prod_{k=1}^{n} \mathcal{O}_{k,\mathrm{micro}}(\sigma_k)\Big\rangle_{\mathcal{S}},\end{aligned} \tag{10}$$

where $\langle\cdots\rangle_{\mathcal{S}}$ is the substrate correlation functional on the fiber. Any coupling among subsystems ("interaction") modifies the joint micro-correlator and thereby the resolved correlator; a measurement is the special case in which one subsystem is engineered to leave a robust macroscopic record.

Proposition 1 (No separate collapse postulate) *Given the kernel formalism and Eq. (10), no additional "collapse" dynamics is required. What is colloquially termed "wavefunction collapse" is the update of the* resolved *state induced by: (i) the interaction-driven change of the micro-correlator on* $\mathcal{S}$*, and (ii) the conditioning associated with macroscopic record degrees of freedom. Thus, observation introduces no extra propagating field and remains consistent with UNI-MET and GA0.*

Remarks. (i) The identification observation ≡ interaction ensures that all empirical events are treated within the same resolution calculus; there is no dual ontology. (ii) Conservation laws and Ward identities apply uniformly: BRST/diffeomorphism constraints act on the correlators that feed Eq. (10), so gauge consistency is preserved under resolution. (iii) In practice, coarse-graining the recorder subsystem defines conditional correlators (pointer sectors); Eq. (10) then yields Born-rule weights as relative resolutions encoded by W.

C. Variational derivation of the kernel

To upgrade beyond toy choices, we derive admissible kernels as extrema of a local functional consistent with UNI-MET, GA0, GA2 and CB∞. Consider

$$\begin{aligned}S[W,\lambda] = \int_{\mathcal{M}} \sqrt{-g}\, \mathrm{d}^4x \Bigg[&\int_{\mathcal{S}} \mathrm{d}\mu(\sigma)\, \mathcal{L}\big(W, \nabla_x W, \nabla_\sigma W\big) \\ &+\; \lambda(x)\Big(\int_{\mathcal{S}} W\, \mathrm{d}\mu - 1\Big)\Bigg],\end{aligned} \tag{11}$$

with a local, positive, causal density $\mathcal{L}$. A minimal, symmetry-respecting choice is

$$\mathcal{L} = \frac{\alpha}{2}\, g^{\mu\nu}\, \partial_\mu W\, \partial_\nu W + \frac{\beta}{2}\, \gamma^{AB}\, \nabla_A W\, \nabla_B W + \xi\, W \ln W, \tag{12}$$

where γ_{AB} is a reference Riemannian metric on $\mathcal{S}$ (induced from $\mathcal{S}_{\mathrm{base}}$), $\alpha, \beta > 0$ set spacetime/fiber resolution penalties, and the entropic term $W \ln W$ enforces positivity and selects a unique normalized representative.

Varying W with fixed $g_{\mu\nu}$ and γ_{AB} yields the Euler–Lagrange equation

$$-\alpha\, \Box W \;-\; \beta\, \Delta_\sigma W \;+\; \xi\,(1 + \ln W) \;=\; \lambda(x), \tag{13}$$

Reflective events: input → projection → output. At each spacetime point x we treat physics as a *local reflective event*:

- **Input (GR & substrate).** Local GR state (metric, matter sources) + local substrate state $W(x,\cdot)$.
- **Projection (causal, local).** A projector at x combines these inputs and produces observable content.

- **Output (to next step).** Updated observables at x and an updated $W(x,\cdot)$; these flow forward along light cones and become inputs at nearby points.

In shorthand:

$$(\text{GR at } x,\ W_x) \xrightarrow{\text{project}} (\mathcal{O}_x,\ W_x^{\text{new}}),$$

with the update constrained by causality (no superluminal signalling). Where fields are strong, the local resolution length $\ell_{\text{res}}(x)$ shrinks and the substrate behaves like a *mirror*: short–distance structure is filtered, while macroscopic GR evolution remains deterministic. Whether one pictures an "inside-sphere" or "external" projection is immaterial—the same W_x gives the same outputs at x.

Numerical method at a glance. For stationary runs on S^3 we discretize the zonal coordinate with the exact S^3 measure and use a divergence–form Laplacian. We solve Eq. (13) with a projected–Newton step in W (augmented constraint row, line search to enforce $W > 0$), reporting weighted residuals and information–theoretic deviations from $W_0 = 1/(2\pi^2)$. This validates the existence/uniqueness results and provides explicit, non–toy structured kernels used in the Yukawa section.

Numerical status (stationary S^3). We implemented a projected-Newton solver with positivity, normalization, and backtracking line search (App. A). Converged runs produce positive, normalized $W(\chi)$ profiles for zonal biases and agree under grid/tolerance changes. Representative diagnostics and profiles are provided in App. A; full physical $W(x,\sigma)$ solutions will be presented separately.

Well-posedness: hyperbolicity, existence, regularity

Assumptions (A1–A4). (A1) $(M, g_{\mu\nu})$ is globally hyperbolic with smooth Cauchy slices; (A2) the fiber (S, γ_{AB}) is compact, smooth, and without boundary (or with admissible Neumann/even Klein data); (A3) $\alpha, \beta, \xi > 0$ are fixed constants in Eq. (13); (A4) admissible initial data $\{W|_{\Sigma_0}, \partial_t W|_{\Sigma_0}\} \in H^1_x H^1_\sigma \times L^2_x H^1_\sigma$ obey normalization $\int_S W\, d\mu = 1$ and $W \geq 0$ a.e.

Theorem 2 (Luminal characteristics) *For fixed $\sigma \in S$, the x-kinetic part of Eq. (13) is a linear wave operator with principal symbol $\alpha\, g^{\mu\nu}\xi_\mu\xi_\nu$. Hence characteristics coincide with the null cone of $g_{\mu\nu}$; no superluminal propagation arises (GA0).*

[Sketch] Principal symbol analysis: the highest-derivative x-terms furnish $\alpha\, g^{\mu\nu}\partial_\mu\partial_\nu$, whose characteristic set is $g^{\mu\nu}\xi_\mu\xi_\nu = 0$. Lower-order terms and the elliptic σ-part do not affect the cone.

Theorem 3 (Global existence and uniqueness) *Under (A1–A4), the mixed hyperbolic–elliptic IBVP for Eq. (13) with the normalization constraint admits a unique solution $W \in C^0\big(\mathbb{R}; H^1_x H^1_\sigma\big) \cap C^1\big(\mathbb{R}; L^2_x H^1_\sigma\big)$.*

[Sketch] Energy estimates on globally hyperbolic M control the hyperbolic x-part; coercivity of the elliptic Δ_σ plus compactness of S and the entropic convexity term $\xi\, W \ln W$ yield strict convexity on each slice. The normalization constraint is enforced by a slice-wise Lagrange multiplier $\lambda(x)$; uniqueness follows from strict convexity.

Lemma 1 (Positivity and maximum principle) *With $\xi > 0$ and admissible boundary data (Neumann/even Klein), solutions satisfy $W \geq 0$ and $\int_S W\, d\mu = 1$ for all times; no negative excursions or blow-up occur.*

[Sketch] The entropy barrier renders the functional strictly convex and penalizes $W \to 0^+$. For the σ-elliptic part, apply the maximum principle on compact S; normalization is preserved by construction via $\lambda(x)$.

Well-posedness, existence, and uniqueness. We now make the variational problem rigorous.

Theorem 4 (Kernel theorem) *Fix $\alpha, \beta, \xi > 0$, and let $\mathcal{S}$ be a compact fiber with smooth Riemannian metric γ_{AB}. For each $x \in \mathcal{M}$, the minimization*

$$\min_{W \in \mathcal{A}_x} \int_{\mathcal{S}} \Big(\tfrac{\alpha}{2}\, g^{\mu\nu}\partial_\mu W\, \partial_\nu W + \tfrac{\beta}{2}\, \gamma^{AB} \nabla_A W\, \nabla_B W + \xi\, W \ln W \Big)\, d\mu(\sigma) \tag{14}$$

subject to $\int_{\mathcal{S}} W\, d\mu = 1$ and $W \geq 0$ admits a unique solution ...

[Proof sketch] (Direct method of the calculus of variations.) Coercivity and strict convexity follow from $\alpha, \beta > 0$ (Dirichlet terms) and the strictly convex entropic term $W \ln W$ for $W \geq 0$. Lower semicontinuity holds on $H^1(\mathcal{S})$; the affine constraint defines a weakly closed subset. Existence follows by compactness; strict convexity yields uniqueness. The Euler–Lagrange equation is (13); positivity follows from the entropy barrier (and maximum principle for the elliptic part in σ).

Boundary data and characteristics. On a foliation with non-null boundary $\partial\mathcal{U}_x \subset \mathcal{S}$ (or on a Klein-identified $\mathcal{S}$), admissible W obey either Neumann data $\nabla_n W = 0$ or evenness under the antipodal map; both preserve normalization and ensure well-posedness of (13). By GA0, the characteristic cone of the x-kinetic part is luminal, so W propagates at c in spacetime and diffuses on $\mathcal{S}$.

Numerical check (linearized, $\alpha > 0$). Linearizing Eq. (13) about the uniform solution on S^3 and projecting on a single zonal harmonic $Z_\ell(\chi)$ yields $\alpha(\partial_{tt} - \partial_{xx})a + (\xi + \beta\lambda_\ell)a = 0$ with $\lambda_\ell = \ell(\ell+2)$, so the *characteristic* speed in x is strictly luminal ($c = 1$). A finite–difference evolution of a localized bump confirms a peak–trajectory slope $c_{\text{fit}} \approx 1$, consistent with GA0, while the $(\xi + \beta\lambda_\ell)$ term only contributes a masslike oscillation factor.

Corollary 1 (Born weights as relative resolutions) *Let $\{A_i\}$ be a measurable partition of $\mathcal{S}$. Define*

$p_i(x) := \int_{A_i} W(x,\sigma)\, d\mu(\sigma)$. *Then* $p_i \geq 0$ *and* $\sum_i p_i = 1$ *by* (5). *If the micro-correlator factorizes across* $\{A_i\}$, *the resolved n-point function* (10) *reduces to a convex combination with weights* $\{p_i\}$; *these are the Born-rule probabilities for outcomes labeled by the partition.*

with spacetime d'Alembertian $\Box$ and fiber Laplacian Δ_σ. Varying λ enforces the normalization constraint (5). Equation (13) is elliptic in σ and hyperbolic in x; admissible solutions satisfy luminal characteristics (GA0), locality (7) and reparametrization invariance (6).

D. Zeta-aligned substrate hypothesis

We posit that the substrate admits an analytic organization analogous to the Riemann zeta function: a critical line acting as a global orientation and a symmetry across that line pairing substrate modes. The observable world is a projection of this structure: states on the line are preserved (fixed orientation), while states off the line project as ratios and asymmetries (small–large hierarchy, particle/antiparticle). See Axiom 25 for the analytic origin (critical-line inheritance).

Global vs. local alignment: critical line, θ, *and* Φ. There are two equivalent realizations of ZETA–POS in SSC:

- **Option A (global):** The critical line maps to $\theta = 0$ (global vacuum alignment). Symmetry across the line encodes particle/antiparticle pairing; the Φ-neutrality sum rule dynamically re-enforces alignment in projection.

- **Option B (local):** The critical line maps to the elliptic Φ-constraint (slice-wise neutrality). Locking the line locally implements the same global alignment; the nonlocal screening term arises as the projection geometry of that line.

In SSC these are compatible: the critical line provides the deeper structure; θ is its global orientation; Φ is its local enforcement.

Antiparticles and annihilation as projection redundancy. Substrate pairing implies particle and antiparticle are twin modes pre-projection. Annihilation corresponds to converging projections; once coincident, one projection is redundant and the pair reverts to the unprojected, symmetric substrate state.

Higgs angularity and the electroweak hierarchy. Assigning the preserved global angular mode to the Higgs (Axiom 24) becomes a corollary of ZETA–POS: the critical-line orientation is the origin of kernel locking. Fluctuations that would rotate this preserved angle are projected out at leading order; the remaining electroweak and Yukawa effects set a light, stable Higgs mass without partner fields.

Kernel locking of the preserved mode. By Axiom 24, among the angular modes on the substrate fiber we single out one preserved mode. The kernel weights are chosen so that, under coarse-graining on each slice, long-wavelength gradients of this preserved mode average to zero. Operationally, W acts as an orthogonality filter: fluctuations that would rotate the preserved angle are suppressed at leading order in the projected sector, while orthogonal fluctuations are unaffected. This locking condition is global (projection-level) and does not modify the local gauge or BRST structure of the low-energy theory. See Axiom 25 for the analytic origin (critical-line inheritance).

E. Symmetry-reduced solutions and illustrative forms

For a fiber with $S^2 \times S^1$ symmetry or a Klein self-identification of S^3, expand

$$W(x,\sigma) = \sum_{\ell m n} c_{\ell m n}(x)\, Y_{\ell m}(\Omega)\, e^{in\theta}, \tag{15}$$

where (Ω,θ) are angles on $\mathcal{S}$. In stationary patches ($\partial_t c_{\ell m n} = 0$), (13) reduces to

$$\left[\beta(\ell(\ell+1)+n^2)+\xi\right] c_{\ell m n} + \xi\, c_{\ell m n} \ln \bar{W} = \lambda\, c_{\ell m n}, \tag{16}$$

with $\bar{W}$ a local average fixing the normalization. Truncation to lowest harmonics and small-gradient limits yield narrow, approximately Gaussian lobes on $\mathcal{S}$, thereby recovering the practical overlap textures previously used for Yukawas as *illustrative* toy kernels.

F. Consequences for observables

The resolution formalism makes no categorical distinction between "physical interactions" and "measurements": both are instances of Eq. (10). Scattering amplitudes and Born probabilities thus emerge as special cases of the same kernel calculus.

Gauge strengths. With GC–SSC, coarse-grained projectors $P_i(\sigma)$ define

$$\frac{1}{g_i^2(\mu)} = \kappa \int_{\mathcal{S}} d\mu(\sigma)\, P_i(\sigma) \Big[\rho_{\rm res}(x,\sigma) + \beta' \mathcal{K}(x,\sigma)\Big]_\mu W(x,\sigma), \tag{17}$$

where $[\cdot]_\mu$ denotes coarse-graining to scale μ. The ratios and their running become functionals of the *derived* W rather than assumptions.

Scattering amplitudes. For n incoming and m outgoing asymptotic states represented by substrate profiles $\Psi^{\rm in/out}(\sigma)$, the SSC scattering functional is

$$\mathcal{A}_{n\to m} = \int \left[\prod_{\alpha=1}^{n+m} d\mu(\sigma_\alpha)\, W(x_\alpha,\sigma_\alpha)\right] \times \Big\langle \Psi^{\rm out}(\sigma_{n+1},\ldots,\sigma_{n+m})\, \Psi^{\rm in}(\sigma_1,\ldots,\sigma_n)\Big\rangle_{\mathcal{S}}. \tag{18}$$

This is precisely the resolution of the substrate S–matrix element. The kernel supplies the physical weighting; unitarity and Ward identities are inherited from the substrate correlator.

Measurement probabilities. A measurement is the special case in which one subsystem is engineered as a recorder with distinct pointer states $\{R_j\}$, each corresponding to disjoint sectors of the fiber $\mathcal{S}$. The probability of outcome j is

$$p_j = \int_{\mathcal{S}_j} d\mu(\sigma)\, W(x,\sigma)\, \rho_{\text{eff}}(\sigma), \tag{19}$$

with $\rho_{\text{eff}}(\sigma)$ the effective density from entangled micro-correlators. This reproduces the Born rule as relative resolution weights of disjoint sectors.

Cosmological residual (tracking vs. freeze). On the expanding foliation (CB∞), the homogeneous component of W sources a residual

$$\Lambda \sim \frac{8\pi G}{c^2}\Big\langle \rho_{\text{res}} \Big\rangle_{\text{hom}}, \tag{20}$$

with tracking $\Lambda \propto H^2$ when W adiabatically follows H, and freeze-out to an effective constant when $\partial_t W$ decouples at late times. The pair (α, z_*) characterizing the tracking fraction and freeze redshift is thus computable from kernel dynamics.

Flavor hierarchies. Family wavelets $\Psi_i^L(\sigma), \Psi_j^R(\sigma)$ supported by the low-ℓ, n modes yield Yukawas

$$(Y_f)_{ij} \propto \int_{\mathcal{S}} d\mu(\sigma)\, W\, P_H(\sigma)\, \Psi_i^L(\sigma)\, \Psi_j^R(\sigma), \tag{21}$$

replacing heuristic Gaussian overlaps by integrals with W obtained from (13). Hierarchies and mixings follow from relative lobe geometry.

Unification of cases. Both scattering amplitudes and measurement probabilities are integrals of substrate correlators weighted by the kernel W. The former involve dynamical evolution between asymptotic states, while the latter involve conditioning on recorder sectors. In SSC they are not separate postulates but unified manifestations of resolution events.

G. Klein hypersphere and boundary conditions

If $\mathcal{S}$ is a Klein-self-identified hypersphere (antipodal identification $\sigma \sim \mathcal{A}(\sigma)$), admissible kernels obey

$$W(x,\sigma) = W\big(x, \mathcal{A}(\sigma)\big), \qquad \int_{\mathcal{S}} W\, d\mu = 1, \tag{22}$$

selecting even harmonics under the identification. This topological constraint fixes zero-modes uniquely (up to reparametrization) and regularizes large-scale drifts of W. *Remark.* Evenness under the antipodal map is equivalent to imposing Neumann data on the $\mathbb{RP}^n$ quotient; this removes zero-mode drifts while preserving the normalization constraint.

H. Numerical note (for reproducibility)

For practical fits one may solve (13) by projected gradient flow with entropy projection enforcing $W \geq 0$ and (5):

$$\partial_\tau W = \alpha\, \Box W + \beta\, \Delta_\sigma W - \xi\,(1 + \ln W) + \lambda(x), \tag{23}$$

with $\lambda(x)$ updated each step to maintain normalization. Convergence in τ yields the stationary W used for predictions. *Convergence.* Because the functional in Thm. 3 is strictly convex in W under the positivity/normalization constraint, the projected gradient flow converges to the unique stationary solution for each x.

Summary. This section promotes the kernel from a didactic approximation to a derived object fixed by axioms and a minimal variational principle. Toy kernels are recovered as symmetry/zero-gradient limits. The interpretation paragraphs connect the solo state of the quantum sphere to open phase and resolution states, and establish that *interaction, resolution, and observation are equivalent events*, giving the empirical meaning of $W(x,\sigma)$. Scattering amplitudes, measurement probabilities, cosmological residuals, and flavor hierarchies all emerge as unified consequences of this single resolution calculus.

IV. EMERGENCE OF GENERAL RELATIVITY

Having established the SSC axioms and projection kernel (Sec. III), we now show how classical General Relativity emerges from the *core resolution state* as the unique low-energy effective description of the metric sector. The kernel's resolution calculus enforces diffeomorphism invariance, a single luminal cone (GA0), and universal metric coupling (UNI-MET). Locality and second-order equations of motion then single out the Einstein–Hilbert action with its boundary completion; the gravitational constant G is fixed internally by the SSC flux–content relation (GA2). The constraint field Φ eliminates unwanted scalar degrees of freedom.

A. Action, boundary, and uniqueness

Theorem 5 (EH+GHY) (Uniqueness of the 4D metric action from SSC.) *Assume GR-Ω, UNI-MET, diffeomorphism invariance, locality, and that the metric Euler–Lagrange equations are at most second order. Then in four dimensions the unique local bulk action (up to a cosmological constant) is*

$$S_{\text{bulk}} = \frac{1}{16\pi G}\int \sqrt{-g}\, R\, \mathrm{d}^4x,$$

and a well-posed Dirichlet variational problem requires the Gibbons–Hawking–York boundary term

$$S_{\text{bdy}} = \frac{1}{8\pi G}\int_{\partial\mathcal{M}} \sqrt{|h|}\, K\, \mathrm{d}^3y.$$

(i) *Admissible scalars.* Locality and diffeomorphism invariance restrict the bulk Lagrangian to scalar densities built from $g_{\mu\nu}$ and $R_{\mu\nu\rho\sigma}$, i.e. $\sqrt{-g}\, f(R_{\mu\nu\rho\sigma}, g)$.

(ii) *Second-order field equations.* In $D = 4$, demanding at-most second-order metric Euler–Lagrange equations selects the Lovelock densities; the only possibilities are a constant and R. Hence the bulk density is $\sqrt{-g}(\Lambda + R)$ up to normalization.

(iii) *Boundary variation.* Varying the Einstein–Hilbert term yields a bulk piece proportional to $G_{\mu\nu}\delta g^{\mu\nu}$ and a total divergence $\nabla_\mu V^\mu$ (see Eq. (24) below for the explicit V^μ). On a non-null boundary with unit normal n^μ, the surface term is $\int_{\partial\mathcal{M}} \sqrt{|h|}\, n_\mu V^\mu$.

(iv) *GHY completion and Dirichlet data.* The Gibbons–Hawking–York term varies as $\delta S_{\rm bdy} \propto (K_{ab} - K h_{ab})\delta h^{ab} - n_\mu V^\mu$. For Dirichlet boundary data ($\delta h_{ab} = 0$) the first term vanishes and the $-n_\mu V^\mu$ cancels the boundary contribution from the bulk variation, leaving a well-posed variational principle with bulk equations $G_{\mu\nu} = 8\pi G\, T_{\mu\nu}$.

(v) *Normalization via GA2.* The overall coefficient $1/(16\pi G)$ is fixed internally by GA2 (flux = content) in the weak-field limit (Sec. IV.B), matching the Newtonian Gauss law.

Explicit variation and boundary cancellation. For the bulk term:

$$\delta\big(\sqrt{-g}\, R\big) = \sqrt{-g}\, G_{\mu\nu}\, \delta g^{\mu\nu} + \sqrt{-g}\, \nabla_\mu V^\mu, \qquad (24)$$
$$V^\mu := g^{\alpha\beta}\nabla^\mu \delta g_{\alpha\beta} - \nabla_\beta \delta g^{\mu\beta}.$$

Thus

$$\delta S_{\rm EH} = \frac{1}{16\pi G}\int_{\mathcal{M}} \sqrt{-g}\, G_{\mu\nu}\, \delta g^{\mu\nu} + \frac{1}{16\pi G}\int_{\partial\mathcal{M}} \sqrt{|h|}\, n_\mu V^\mu. \qquad (25)$$

The Gibbons–Hawking–York term $S_{\rm GHY} = \frac{1}{8\pi G}\int_{\partial\mathcal{M}} \sqrt{|h|}\, K$ varies as

$$\delta S_{\rm GHY} = \frac{1}{8\pi G}\int_{\partial\mathcal{M}} \sqrt{|h|}\, \big[(K_{ab} - K h_{ab})\, \delta h^{ab} - n_\mu V^\mu\big]. \qquad (26)$$

For Dirichlet data ($\delta h_{ab} = 0$) the $(K_{ab} - K h_{ab})\, \delta h^{ab}$ term vanishes and the $-n_\mu V^\mu$ cancels the boundary piece from $\delta S_{\rm EH}$, leaving a well-posed bulk variation with equations $G_{\mu\nu} = 8\pi G\, T_{\mu\nu}$.

Theorem 6 (Internal normalization of G via GA2) *On a large enclosing 2-sphere S_R in a near-flat patch, GA2 equates the* resolution flux *through S_R to the* content *enclosed, fixing the bulk action coefficient to $1/(16\pi G)$ without Newtonian matching.*

[Uniform sphere example] Consider a static, uniform-density ball of mass M and radius $R_\star \ll R$. Let $\Phi_{\rm res}$ denote the flux functional implied by GA2 from the kernel calculus; in the weak-field limit it reduces to $\oint_{S_R} \nabla_i U\, dS^i$ with U the Newtonian potential. By GA2, $\Phi_{\rm res}(S_R) = 4\pi G M$ equals the integrated content $\int(\rho - \varepsilon)\, d^3x$. Matching the linearized field equation from $S_{\rm grav}$ to $\nabla^2 U = 4\pi G\rho$ fixes the overall coefficient to $1/(16\pi G)$.

Fixing the $1/16\pi G$ coefficient (GA2). In the weak, static limit, write $g_{00} = -1 + 2\Phi_N/c^2$ and $g_{ij} = (1 + 2\Phi_N/c^2)\delta_{ij}$. The linearized Einstein equations give $\nabla^2\Phi_N = 4\pi G\,\rho$. Integrating over a ball B_R enclosing total mass $M = \int_{B_R} \rho\, {\rm d}^3x$ and using Gauss' law:

$$\oint_{S_R} \nabla\Phi_N \cdot {\rm d}\mathbf{S} = 4\pi G\, M. \qquad (27)$$

For a point mass, $\Phi_N = -GM/r$ gives the same surface flux. This is precisely the GA2 "flux = content" statement, and fixes the coupling in the bulk action to be $1/16\pi G$ so that the Newtonian limit reproduces the observed G.

Explicit G normalization example (uniform sphere)

Let $\rho = \rho_0\, \Theta(R - r)$ (static). Solve $\nabla^2\Phi_N = 4\pi G\rho$:

$$\Phi_N(r) = \begin{cases} -2\pi G\rho_0 \left(R^2 - \frac{r^2}{3}\right), & r \le R, \\ -\dfrac{GM}{r}, \quad M = \dfrac{4\pi}{3}\rho_0 R^3, & r \ge R. \end{cases} \qquad (28)$$

Compute the surface flux at any $r \ge R$: $\oint_{S_r} \nabla\Phi_N \cdot {\rm d}\mathbf{S} = 4\pi G M$. Thus GA2 (flux = content) reproduces the same G as the metric sector with the $1/16\pi G$ normalization.

B. Sorting sector and field equations

Sorting sector. Φ is a Lagrange multiplier (Φ-CONST):

$$S_{\rm sort} = \int \sqrt{-g}\, [-\Phi(\rho - \varepsilon)]\, {\rm d}^4x. \qquad (29)$$

Field equations:

$$R_{\mu\nu} - \tfrac{1}{2} R\, g_{\mu\nu} = 8\pi G\, T_{\mu\nu}, \qquad \nabla^2\Phi = 4\pi G(\rho - \varepsilon). \qquad (30)$$

Theorem 7 (Int normalization of G (Gauss law)) *On a large enclosing S_R in a near-flat patch, GA2 equates resolution flux to content, fixing the action coefficient to $1/16\pi G$ internally (no Newtonian matching).* Descriptor: *the same G appears in both Einstein and Poisson sectors.*

Theorem 8 (Ext neutrality of Φ (no scalar hair)) *For $\Phi|_S = 0$ on a smooth 2-surface S enclosing* $\mathrm{supp}(\rho - \varepsilon)$ *and $\Phi \to 0$ at infinity, the unique exterior solution is $\Phi \equiv 0$.* Descriptor: *outside sources, SSC reduces to vacuum (or standard matter) GR.*

Proof (maximum principle & Hopf lemma): Harmonic Φ on $\Omega_{\rm ext}$ attains extrema on $S \cup \{\infty\}$ and both values are zero $\Rightarrow$ $\Phi \equiv 0$. Neumann/Robin variants use outward normal inequalities to force the trivial solution. □

Bianchi & conservation (completeness check). Varying $S_{\rm grav}$ gives $\nabla^\mu G_{\mu\nu} = 0$ (Bianchi); hence $\nabla^\mu T_{\mu\nu} = 0$ on-shell. The Φ-equation is elliptic and does not alter the local conservation law.

C. Hamiltonian analysis and degrees of freedom

ADM split: (h_{ij}, π^{ij}) with lapse N and shift N^i as Lagrange multipliers. The primary constraints are $\pi_N \approx 0$, $\pi_i \approx 0$; varying N, N^i yields the Hamiltonian and momentum constraints,

$$\mathcal{H} = \frac{1}{\sqrt{h}}\Big(\pi_{ij}\pi^{ij} - \tfrac{1}{2}\pi^2\Big) - \sqrt{h}\, R^{(3)} \approx 0, \tag{31a}$$

$$\mathcal{H}_i = -2\,\nabla_j \pi^j{}_i \approx 0. \tag{31b}$$

For the non-propagating constraint field Φ we have a second-class pair $(\pi_\Phi, \mathcal{C}_\Phi)$ eliminated by the Dirac bracket; no Φ-mode propagates. The remaining constraints close under the Dirac (Poisson) bracket as in GR,

$$\begin{aligned}\{\mathcal{H}[\alpha], \mathcal{H}[\beta]\} &= \mathcal{H}_i\big[h^{ij}(\alpha\partial_j\beta - \beta\partial_j\alpha)\big]\,,\\ \{\mathcal{H}_i[\xi^i], \mathcal{H}[\alpha]\} &= \mathcal{H}[\mathcal{L}_\xi\alpha],\\ \{\mathcal{H}_i[\xi^i], \mathcal{H}_j[\eta^j]\} &= \mathcal{H}_i[(\mathcal{L}_\xi\eta)^i].\end{aligned} \tag{32}$$

so the theory has exactly two propagating tensor polarizations.

Result. SSC gravity $\Rightarrow$ 2 propagating DOF, no extra scalar or vector modes.

D. Linear waves (bridge to full treatment)

Linearizing the metric about Minkowski, $g_{\mu\nu} = \eta_{\mu\nu} + h_{\mu\nu}$, and imposing harmonic gauge $\partial^\mu \bar{h}_{\mu\nu} = 0$ with $\bar{h}_{\mu\nu} := h_{\mu\nu} - \frac{1}{2}\eta_{\mu\nu}h$, the field equations reduce to the standard sourced wave equation

$$\Box \bar{h}_{\mu\nu} = -\frac{16\pi G}{c^4}\, T_{\mu\nu}. \tag{33}$$

By GA0 (single luminal cone) and Φ-CONST (non-propagating constraint), disturbances propagate at c with exactly two tensor polarizations and no scalar radiation channel. We defer the full mode decomposition, energy flux, and observational phenomenology to Sec. VI.

Ghosts and causality. The metric field equations are second order and single-metric; no higher-derivative curvature densities are introduced in the low-energy sector, so there is no Ostrogradsky instability. Linearized constraints eliminate non-tensor modes (Sec. V), and the characteristic cone coincides with c (Thm. 2), precluding superluminal or acausal propagators.

E. Post-Newtonian expansion (bridge to full treatment)

Beyond the Newtonian limit, the SSC framework admits a systematic post-Newtonian (PN) expansion in powers of v/c or $GM/(rc^2)$. The structure is identical to that of GR, producing corrections at 1PN order consistent with the Einstein–Infeld–Hoffmann (EIH) equations. We defer the full derivation, including explicit 1PN dynamics and observable consequences (perihelion shift, Shapiro delay), to Sec. IV E.

F. N-body dynamics and periastron

From the 1PN metric one recovers the standard Einstein–Infeld–Hoffmann N-body Lagrangian, including the triple-mass terms mapping back to nonlinearities in g_{00}. For binaries this yields the canonical periastron advance:

$$\Delta\omega = \frac{6\pi GM}{a(1-e^2)c^2}, \tag{34}$$

matching GR.

Summary. Starting from the SSC axioms and projection kernel, the emergent metric sector reproduces General Relativity in full detail: EH+GHY action, correctly normalized G, two tensor DOF, luminal propagation, 1PN expansion, and N-body dynamics.

V. FULL ADM/DIRAC ANALYSIS

ADM decomposition $ds^2 = -N^2dt^2 + h_{ij}(dx^i + N^i dt)(dx^j + N^j dt)$. Momenta $\pi^{ij} = \frac{\sqrt{h}}{16\pi G}(K^{ij} - Kh^{ij})$. Primary constraints: $\pi_N \approx 0$, $\pi_i \approx 0$, $\pi_\Phi \approx 0$. Hamiltonian (up to boundary):

$$H = \int \mathrm{d}^3x\, (N\mathcal{H} + N^i\mathcal{H}_i + \lambda_\Phi\pi_\Phi), \tag{35}$$

$$\begin{aligned}\mathcal{H} &= \frac{16\pi G}{\sqrt{h}}(\pi_{ij}\pi^{ij} - \tfrac{1}{2}\pi^2) - \frac{\sqrt{h}}{16\pi G}\,{}^{(3)}R\\ &\quad + \sqrt{h}\,\Phi(\rho - \varepsilon) + \mathcal{H}_{\rm matter},\end{aligned} \tag{36}$$

$$\mathcal{H}_i = -2\,\nabla_j\pi^j{}_i + \mathcal{H}_i^{\rm matter}. \tag{37}$$

Secondary: $\mathcal{H} \approx 0$, $\mathcal{H}_i \approx 0$, $\mathcal{C}_\Phi := \sqrt{h}(\rho - \varepsilon) - \sqrt{h}\nabla^2\Phi/(4\pi G) \approx 0$.

Algebra and DOF. $\{\mathcal{H}, \mathcal{H}\}, \{\mathcal{H}_i, \mathcal{H}\}, \{\mathcal{H}_i, \mathcal{H}_j\}$ close as in GR (first class). $\{\pi_\Phi(x), \mathcal{C}_\Phi(y)\} = \frac{\sqrt{h}}{4\pi G}\nabla_x^2\delta^{(3)}(x-y)$ is invertible $\Rightarrow$ second-class pair. Dirac-bracket eliminate $(\pi_\Phi, \mathcal{C}_\Phi)$. Remaining: 2 configuration DOF (tensor polarizations). No scalar propagator.

Dirac bracket for the $(\pi_\Phi, \mathcal{C}_\Phi)$ pair. Primary constraint $\pi_\Phi \approx 0$ and secondary $\mathcal{C}_\Phi := \nabla^2\Phi - 4\pi G(\rho - \varepsilon) \approx 0$ form a second-class pair with

$$\{\pi_\Phi(\mathbf{x}), \mathcal{C}_\Phi(\mathbf{y})\} = \nabla^2\delta^{(3)}(\mathbf{x} - \mathbf{y}).$$

Let $G(\mathbf{x},\mathbf{y})$ be the Green operator satisfying $\nabla^2 G(\mathbf{x},\mathbf{y}) = \delta^{(3)}(\mathbf{x}-\mathbf{y})$ with the same boundary data as Φ. The Dirac bracket for any functionals F, G is

$$\begin{aligned}\{F,G\}_D &= \{F,G\} \\ &\quad - \int \mathrm{d}^3u\,\mathrm{d}^3v\,\{F,\pi_\Phi(\mathbf{u})\}\,G(\mathbf{u},\mathbf{v})\,\{\mathcal{C}_\Phi(\mathbf{v}),G\} \\ &\quad + \ (\pi_\Phi \leftrightarrow \mathcal{C}_\Phi). \end{aligned} \tag{38}$$

Since h_{ij}, π^{ij} have vanishing Poisson brackets with π_Φ and $\mathcal{C}_\Phi$, their Dirac brackets equal their Poisson brackets. Thus eliminating (Φ,π_Φ) leaves the standard GR phase space and symplectic structure.

Constraint algebra and DOF count

With smearing functions,

$$H[N] = \int \mathrm{d}^3x\, N\,\mathcal{H}, \qquad H[\vec{N}] = \int \mathrm{d}^3x\, N^i\,\mathcal{H}_i,$$

the (Dirac) algebra closes as in GR:

$$\{H[\vec{N}], H[\vec{M}]\} = H[\mathcal{L}_{\vec{N}}\vec{M}], \tag{39}$$

$$\{H[\vec{N}], H[M]\} = H[\mathcal{L}_{\vec{N}}M], \tag{40}$$

$$\{H[N], H[M]\} = H_i\big[h^{ij}(N\partial_j M - M\partial_j N)\big]\,. \tag{41}$$

The Φ-pair is second-class and removed as in the previous subsection; it does not alter the first-class subalgebra above.

Degrees of freedom. Canonical variables per point: (h_{ij},π^{ij}) (12), (N,π_N) (2), (N^i,π_i) (6), (Φ,π_Φ) (2) $\Rightarrow$ 22. Constraints: 8 first-class $(\pi_N,\pi_i,\mathcal{H},\mathcal{H}_i)$ and 2 second-class $(\pi_\Phi,\mathcal{C}_\Phi)$. Thus

$$\#\mathrm{DOF} = \tfrac{1}{2}\,[22 - 2\times 8 - 2] = 2,$$

the two tensor polarizations of GR.

VI. LINEAR WAVES

Linearize $g_{\mu\nu} = \eta_{\mu\nu} + h_{\mu\nu}$, harmonic gauge $\partial^\mu \bar{h}_{\mu\nu} = 0$ with $\bar{h}_{\mu\nu} = h_{\mu\nu} - \frac{1}{2}\eta_{\mu\nu}h$:

$$\Box \bar{h}_{\mu\nu} = -\frac{16\pi G}{c^4} T_{\mu\nu}.$$

By GA0, waves are luminal; (Φ-CONST) forbids scalar radiation.

VII. POST-NEWTONIAN EXPANSION TO 1PN (FULL BOOKKEEPING)

We solve Einstein's equations iteratively in powers of $\epsilon \sim v/c \sim \sqrt{U}/c$.

A. Matter model and PN scalings

For a perfect fluid with rest density ρ, internal energy per mass Π, pressure p:

$$T^{00} = \rho c^2\left(1 + \Pi + \frac{v^2}{c^2} + \mathcal{O}(\epsilon^4)\right), \tag{42}$$

$$T^{0i} = \rho c\, v^i\left(1 + \Pi + \frac{v^2}{c^2} + \frac{p}{\rho c^2}\right) + \mathcal{O}(\epsilon^5), \tag{43}$$

$$T^{ij} = \rho v^i v^j + \delta^{ij} p + \mathcal{O}(\epsilon^4). \tag{44}$$

Define the standard PN potentials (integrals over instantaneous matter distribution):

$$U(\mathbf{x}) = G\int \frac{\rho(\mathbf{x}')}{|\mathbf{x}-\mathbf{x}'|}\,\mathrm{d}^3x', \tag{45}$$

$$V_i(\mathbf{x}) = G\int \frac{\rho(\mathbf{x}')\,v_i(\mathbf{x}')}{|\mathbf{x}-\mathbf{x}'|}\,\mathrm{d}^3x', \tag{46}$$

$$\Phi_1(\mathbf{x}) = G\int \frac{\rho(\mathbf{x}')\,v'^2}{|\mathbf{x}-\mathbf{x}'|}\,\mathrm{d}^3x', \tag{47}$$

$$\Phi_2(\mathbf{x}) = G\int \frac{\rho(\mathbf{x}')\,U(\mathbf{x}')}{|\mathbf{x}-\mathbf{x}'|}\,\mathrm{d}^3x', \tag{48}$$

$$\Phi_3(\mathbf{x}) = G\int \frac{\rho(\mathbf{x}')\,\Pi(\mathbf{x}')}{|\mathbf{x}-\mathbf{x}'|}\,\mathrm{d}^3x', \tag{49}$$

$$\Phi_4(\mathbf{x}) = G\int \frac{p(\mathbf{x}')}{|\mathbf{x}-\mathbf{x}'|}\,\mathrm{d}^3x'. \tag{50}$$

From wave equation to 1PN metric

In harmonic gauge, $\partial_\mu \bar{h}^{\mu\nu} = 0$ with $\bar{h}_{\mu\nu} := h_{\mu\nu} - \frac{1}{2}\eta_{\mu\nu}h$,

$$\begin{aligned}\Box \bar{h}^{\mu\nu} &= -\frac{16\pi G}{c^4}\,\tau^{\mu\nu}, \\ \bar{h}^{\mu\nu}(t,\mathbf{x}) &= \frac{4G}{c^4}\int \frac{\tau^{\mu\nu}(t-|\mathbf{x}-\mathbf{x}'|/c,\mathbf{x}')}{|\mathbf{x}-\mathbf{x}'|}\,\mathrm{d}^3x'.\end{aligned} \tag{51}$$

At 1PN accuracy (slow motion, weak field), the needed potentials are

$$\begin{aligned}U(\mathbf{x}) &= G\int \frac{\rho(\mathbf{x}')}{|\mathbf{x}-\mathbf{x}'|}\,\mathrm{d}^3x', \\ V^i(\mathbf{x}) &= G\int \frac{\rho(\mathbf{x}')\,v^i(\mathbf{x}')}{|\mathbf{x}-\mathbf{x}'|}\,\mathrm{d}^3x'.\end{aligned} \tag{52}$$

Iterating once gives

$$\begin{aligned}g_{00} &= -1 + \frac{2U}{c^2} - \frac{2U^2}{c^4} + \mathcal{O}(c^{-6}), \\ g_{0i} &= -\frac{4V_i}{c^3} + \mathcal{O}(c^{-5}), \\ g_{ij} &= \left(1 + \frac{2U}{c^2}\right)\delta_{ij} + \mathcal{O}(c^{-4}).\end{aligned} \tag{53}$$

which yields $\gamma = \beta = 1$ by direct read-off.

B. Harmonic-gauge field equations at 1PN

Write $g_{\mu\nu} = \eta_{\mu\nu} + h_{\mu\nu}$ and solve $\Box\bar{h}^{\mu\nu} = -\frac{16\pi G}{c^4}\tau^{\mu\nu}$ with $\tau^{\mu\nu} = T^{\mu\nu} + \mathcal{O}(hT)$. Iterating with the flat-space Green's function and enforcing $\partial_\mu\bar{h}^{\mu\nu} = 0$, we obtain the 1PN metric (GR values):

$$g_{00} = -1 + \frac{2U}{c^2} - \frac{2U^2}{c^4} + \frac{4\Phi_1 + 4\Phi_2 + 2\Phi_3 + 6\Phi_4}{c^4} + \mathcal{O}(\epsilon^6), \tag{54}$$

$$g_{0i} = -\frac{4V_i}{c^3} + \mathcal{O}(\epsilon^5), \tag{55}$$

$$g_{ij} = \left(1 + \frac{2U}{c^2}\right)\delta_{ij} + \mathcal{O}(\epsilon^4). \tag{56}$$

These expressions follow by iterating $\Box\,\bar{h}_{\mu\nu} = -16\pi G c^{-4}\tau_{\mu\nu}$ with the flat Green's function under $\partial_\mu\bar{h}^{\mu\nu} = 0$ and matching to the standard PN potentials (U, Φ_a, V_i) with SSC matter scalings.

C. PPN parameters and checks

Comparing (56) to the standard PPN form $g_{ij} = (1 + 2\gamma U/c^2)\delta_{ij}$ gives $\gamma = 1$. Comparing (54) to $g_{00} = -1 + 2U/c^2 - 2\beta U^2/c^4 + \ldots$ yields $\beta = 1$. Absence of a long-range scalar (Φ non-propagating) $\Rightarrow$ no -1PN dipole term in radiation.

PPN parameters beyond γ, β

Because the theory is single-metric, diffeomorphism invariant, and conserves $T^{\mu\nu}$, the preferred-frame and nonconservative parameters vanish:

$$\alpha_1 = \alpha_2 = \alpha_3 = \xi = \zeta_1 = \zeta_2 = \zeta_3 = \zeta_4 = 0.$$

Thus the full PPN set matches GR in screened regimes.

No $-1PN$ dipole radiation. With a single metric and conserved $T^{\mu\nu}$, the monopole is constant and the mass dipole's second derivative equals the total force (zero in the center-of-mass frame). No extra long-range scalar exists to source a -1PN channel, so the leading radiation is quadrupolar,

$$\dot{E}_{\rm GW} = -\frac{G}{5c^5}\left\langle \dddot{Q}_{ij}\dddot{Q}^{ij}\right\rangle.$$

D. Energy flux (quadrupole) and two-body dynamics

At leading PN order the luminosity is

$$\dot{E}_{\rm GW} = -\frac{G}{5c^5}\left\langle \ddddot{Q}_{ij}\ddddot{Q}_{ij}\right\rangle,$$

with Q_{ij} the trace-free mass quadrupole of the source. For a compact binary with separation $\mathbf{r} = \mathbf{x}_1 - \mathbf{x}_2$, reduced mass μ, total mass M, the leading phasing matches GR (no dipole).

E. Periastron advance (1PN)

From the 1PN geodesic/eff. two-body Hamiltonian, the secular periastron advance per orbit is

$$\Delta\omega = \frac{6\pi GM}{a(1-e^2)c^2},$$

for semi-major axis a and eccentricity e (test limit; for comparable masses M is replaced by appropriate total mass entering the 1PN equations of motion). This matches the canonical GR value, confirming SSC $\Rightarrow$ GR at 1PN.

VIII. STANDARD MODEL: GROUP AND CHARGES (WITH EXPLICIT RREF)

Square system (linear + cubic) and RREF. Unknowns $Y^\top = (Y_{q_L}, Y_{u_R}, Y_{d_R}, Y_{\ell_L}, Y_{e_R})$. From $Q = T_3 + Y$ we have $Y_{q_L} = \frac{1}{6}$. Linear anomalies:

$$[SU(2)]^2U(1): \quad 3Y_{q_L} + Y_{\ell_L} = 0, \tag{57}$$

$$[SU(3)]^2U(1): \quad 2Y_{q_L} - Y_{u_R} - Y_{d_R} = 0, \tag{58}$$

$$\text{grav}\text{–}U(1): \quad 6Y_{q_L} - 3Y_{u_R} - 3Y_{d_R} + 2Y_{\ell_L} - Y_{e_R} = 0. \tag{59}$$

Insert $Y_{q_L} = \frac{1}{6}$:

$$Y_{\ell_L} = -\tfrac{1}{2}, \qquad Y_{e_R} = -1, \qquad Y_{u_R} + Y_{d_R} = \tfrac{1}{3}.$$

Cubic anomaly:

$$6Y_{q_L}^3 - 3Y_{u_R}^3 - 3Y_{d_R}^3 + 2Y_{\ell_L}^3 - Y_{e_R}^3 = 0 \;\Rightarrow\; Y_{u_R}^3 + Y_{d_R}^3 = \tfrac{7}{27}. \tag{60}$$

Let $s = Y_{u_R} + Y_{d_R} = \frac{1}{3}$ and $p = Y_{u_R}Y_{d_R}$. Then $s^3 - 3ps = \frac{7}{27} \Rightarrow p = -\frac{2}{9}$. Solve $t^2 - st + p = 0$ to obtain $t \in \{\frac{2}{3}, -\frac{1}{3}\}$. Thus

$$Y_{u_R} = \tfrac{2}{3}, \qquad Y_{d_R} = -\tfrac{1}{3}, \qquad Y_{\ell_L} = -\tfrac{1}{2}, \qquad Y_{e_R} = -1.$$

Uniqueness: the RREF of the linear system (57)–(59) with $Y_{q_L} = \frac{1}{6}$ leaves a one-parameter family; the cubic fixes it uniquely to the above solution.

IX. EMERGENCE OF THE STANDARD MODEL: GROUP, CHARGES, AND MASSES

With the SSC projection kernel $W(x, \sigma)$ established (Sec. III), the low-energy gauge structure is constrained by three ingredients: (i) **universal metric coupling** and a single luminal cone (UNI-MET, GA0), (ii) **admissible, anomaly-free, renormalizable matter sets** (CONS1) consistent with a single visible abelian

factor (AM1) and compact nonabelian factors (NA-low), and (iii) **resolution weights on the fiber** supplied by W, which determine coarse-grained gauge strengths via GC–SSC and encode flavor data through overlap integrals.

Points (i)–(ii) restrict the gauge group and quantum numbers. Point (iii) determines *how strongly* each channel couples and *how fermion masses/mixings arise*, once the minimal Higgs projection channel (HIGGS-PROJ) is specified. In this section we first derive the unique low-energy group and one-generation hypercharges, and then show how Yukawa textures follow from the *derived* kernel W (with the previous toy overlaps appearing as symmetry limits).

Theorem 9 (Low-energy group and hypercharges) *Under AM1, NA-low, CONS1, and CHARGE1, the low-energy gauge group is $G_{\rm SM} = SU(3)_c \times SU(2)_L \times U(1)_Y$, and the unique one-generation hypercharges are*

$$Y_{q_L} = \tfrac{1}{6}, \quad Y_{u_R} = \tfrac{2}{3}, \quad Y_{d_R} = -\tfrac{1}{3}, \quad Y_{\ell_L} = -\tfrac{1}{2}, \quad Y_{e_R} = -1.$$

Descriptor: *necessity of an abelian factor and cubic/linear anomaly cancellation fix the pattern.*

Square system (linear + cubic) and RREF. Unknowns $Y^\top = (Y_{q_L}, Y_{u_R}, Y_{d_R}, Y_{\ell_L}, Y_{e_R})$. From $Q = T_3 + Y$: $Y_{q_L} = \frac{1}{6}$. Linear anomalies:

$$[SU(2)]^2U(1) : 3Y_{q_L} + Y_{\ell_L} = 0, \tag{61}$$

$$[SU(3)]^2U(1) : 2Y_{q_L} - Y_{u_R} - Y_{d_R} = 0, \tag{62}$$

$$\text{grav}\text{–}U(1) : 6Y_{q_L} - 3Y_{u_R} - 3Y_{d_R} + 2Y_{\ell_L} - Y_{e_R} = 0. \tag{63}$$

Insert $Y_{q_L} = 1/6 \Rightarrow Y_{\ell_L} = -1/2 \Rightarrow Y_{e_R} = -1$. Equation (62) gives $Y_{u_R} + Y_{d_R} = 1/3$. The cubic anomaly

$$6Y_{q_L}^3 - 3Y_{u_R}^3 - 3Y_{d_R}^3 + 2Y_{\ell_L}^3 - Y_{e_R}^3 = 0$$

becomes $Y_{u_R}^3 + Y_{d_R}^3 = \frac{7}{27}$. With $s = Y_{u_R} + Y_{d_R} = 1/3$ and $p = Y_{u_R}Y_{d_R}$: $s^3 - 3ps = 7/27 \Rightarrow p = -2/9$. Solve $t^2 - st + p = 0 \Rightarrow t = \{2/3, -1/3\}$. Unique real solution.

Necessity of $U(1)$. If $Q \propto T_3$ only, $Q(u_L) = -Q(d_L)$ contradicts $(+2/3, -1/3)$. Hence the abelian factor is required (CHARGE1).

X. STANDARD MODEL LAGRANGIAN FROM SSC AXIOMS (DERIVED AND UNIQUE)

Setup from axioms. From AM1, NA-low, CONS1, and CHARGE1 (Secs. II, VII), the low-energy gauge group and one-generation hypercharges are fixed: $G_{\rm SM} = SU(3)_c \times SU(2)_L \times U(1)_Y$ and $Y_{q_L} = \frac{1}{6}, Y_{u_R} = \frac{2}{3}, Y_{d_R} = -\frac{1}{3}, Y_{\ell_L} = -\frac{1}{2}, Y_{e_R} = -1$. Fermion content per generation: $q_L \sim (3,2)_{1/6}$, $u_R \sim (3,1)_{2/3}$, $d_R \sim (3,1)_{-1/3}$, $\ell_L \sim (1,2)_{-1/2}$, $e_R \sim (1,1)_{-1}$. Higgs: $\phi \sim (1,2)_{+1/2}$ (HIGGS-PROJ, MASS-PRIOR, CONS1).

Theorem 10 ***Gauge structure and kinetic terms.*** *Local gauge redundancy with compact factors and power counting (CONS1) uniquely fixes the Yang–Mills kinetic terms and minimal couplings:*

$$\mathcal{L}_{\rm gauge} = -\frac{1}{4}G^a_{\mu\nu}G^{a\mu\nu} - \frac{1}{4}W^i_{\mu\nu}W^{i\mu\nu} - \frac{1}{4}B_{\mu\nu}B^{\mu\nu},$$

with field strengths $G^a_{\mu\nu}, W^i_{\mu\nu}, B_{\mu\nu}$ and covariant derivative $D_\mu = \partial_\mu - ig_3T^aG^a_\mu - ig_2\tau^iW^i_\mu - ig_YYB_\mu$.

Fermion sector (minimal coupling).

$$\mathcal{L}_{\rm ferm} = \sum_\psi \bar\psi\, i\gamma^\mu D_\mu \psi \quad \text{for } \psi \in \{q_L, u_R, d_R, \ell_L, e_R\}.$$

Higgs sector (renormalizable, gauge invariant).

$$\mathcal{L}_H = (D_\mu\phi)^\dagger(D^\mu\phi) - \mu^2\,\phi^\dagger\phi - \lambda(\phi^\dagger\phi)^2, \qquad \phi \sim (1,2)_{+1/2}. \tag{64}$$

Lemma 2 ***Yukawa uniqueness at $d \le 4$.*** *Given the chiral assignments above and gauge invariance, the only renormalizable fermion–Higgs couplings are*

$$\mathcal{L}_Y = -\,\bar q_L\, Y_u\, \tilde\phi\, u_R - \,\bar q_L\, Y_d\, \phi\, d_R - \,\bar\ell_L\, Y_e\, \phi\, e_R + h.c.,$$

with $\tilde\phi = i\sigma^2\phi^*$. No other $d \le 4$ gauge-invariant, Lorentz-invariant fermion operators exist.

Higgs as carrier of the preserved mode. Consistent with minimality (HIGGS-PROJ, MASS-PRIOR) and Axiom 24, the Higgs doublet is assigned as the unique low-energy carrier of the preserved angular mode. This assignment leaves the renormalizable SM operator basis unchanged, but explains the stability of the Higgs mass parameter against leading hard sensitivity: the locked mode cannot be tilted by projection of short-wavelength fluctuations.

The assignment follows from ZETA–POS: the preserved line supplies the unique global angular mode. *Proof (sketch).* List all fermion bilinears $\bar\psi_L\phi\psi_R$ and $\bar\psi_L\tilde\phi\psi_R$; require invariance under each factor of $G_{\rm SM}$. Color invariance forces $\bar q_L(\cdots)u_R$, $\bar q_L(\cdots)d_R$ singlets only via color contraction. Weak $SU(2)$ invariance requires doublet–doublet $\to$ singlet via ϵ_{ij} for $\tilde\phi$, or δ_{ij} for ϕ. Hypercharge conservation fixes the three structures written; any alternative choice fails Y-sum or $SU(2)$ index contraction. Quartic/derivative fermion operators are $d > 4$ (forbidden by CONS1). □

SSC–CP selection rule. Convention. Under CP, Φ is odd and $\mathcal{Q}_{\rm top}$ is odd, so $\Phi\,\mathcal{Q}_{\rm top}$ is CP–even. Consequently, a bare $\theta\, G\tilde G$ term is not admitted in $S_{\rm SM}$; the only topological coupling is through the sorting sector, Eqs. (3)–(4).

Strong–CP neutrality (SSC feedback) and axial clean–up. By Axiom 23 and the neutrality sum rule (87), the global contribution of the QCD topological density is erased in screened regimes, implying $\theta_{\rm QCD} \to 0$

without introducing new propagating fields. The physical strong–CP parameter is

$$\bar{\theta} \;\equiv\; \theta_{\rm QCD} + \arg\det M_q,$$

with M_q the quark mass matrix formed from the Yukawas in $\mathcal{L}_Y$. As in standard field theory, an overall anomalous $U(1)_A$ rephasing of quark fields can be chosen to remove $\arg\det M_q$, while the relative left–right misalignment responsible for the CKM phase is unaffected.

Corollary 2 ***Strong–CP neutrality in SSC.*** *Under Axiom 23 and (87), the gauge vacuum angle satisfies $\theta_{\rm QCD} \to 0$ in screened regimes. Choosing the overall anomalous $U(1)_A$ rotation to set $\arg\det M_q = 0$ then yields $\bar{\theta} = 0$, while preserving the CKM source of weak CP violation.*

Proof (sketch). Axiom 23 extends the Φ-constraint source by $\mathcal{Q}_{\rm top}$; exterior neutrality enforces the sum rule (87), which cancels the net topological angle, $\theta_{\rm QCD} \to 0$. The remaining phase $\arg\det M_q$ is removed by the overall anomalous $U(1)_A$ rephasing. Since the CKM phase resides in the relative biunitary misalignment of Y_u, Y_d, it survives unchanged.

Electroweak symmetry breaking (EWSB) and masses. For $\mu^2 > 0$, $\langle\phi\rangle = (0, v/\sqrt{2})^\top$ with $v = \sqrt{\mu^2/\lambda}$. Define $W^\pm = (W^1 \mp i W^2)/\sqrt{2}$, and $A_\mu = \sin\theta_W\, W^3_\mu + \cos\theta_W\, B_\mu$ with $\tan\theta_W = g_Y/g_2$. Mass relations:

$$M_W = \tfrac{1}{2} g_2 v, \quad M_Z = \tfrac{1}{2} v\sqrt{g_2^2 + g_Y^2}, \quad A_\mu \text{ massless},$$
$$Q = T_3 + Y.$$

Proposition 2 (BEH via θ–Φ alignment) *In SSC, gauge bosons whose background-field directions would rotate the preserved angular mode (ANG–POS) are resisted by the elliptic Φ constraint and acquire mass (W, Z). The unbroken combination (photon) is aligned with the θ–Φ gyroscope and remains massless.*

Interpretation. The Higgs doublet carries the preserved mode (ANG–POS). The Φ sector supplies local enforcement (slice-wise locking), while θ provides the global orientation (neutralized). Massiveness = "tries to tilt the preserved angle"; masslessness = "passes through without torque."

Fermion masses: $m_u = Y_u\, v/\sqrt{2}$, $m_d = Y_d\, v/\sqrt{2}$, $m_e = Y_e\, v/\sqrt{2}$ (generation matrices diagonalized by biunitaries; CKM/PMNS from misalignment).

Accidental symmetries and CP phases. At $d \le 4$ the renormalizable SM Lagrangian enjoys accidental global $U(1)_B$ and $U(1)_L$ symmetries. Baryon/lepton violation first appears at $d = 6$ (e.g. $QQQL/\Lambda^2$) and $d = 5$ (Weinberg operator), respectively. Complex Yukawas contain physical CP phases: for three generations, one CKM Dirac phase (quarks) and, for Majorana neutrinos, two additional Majorana phases in PMNS.

Proposition 3 ***Completeness at*** $d \le 4$. *With the field content above, all Lorentz- and gauge-invariant renormalizable operators are exhausted by $\mathcal{L}_{\rm gauge} + \mathcal{L}_{\rm ferm} + \mathcal{L}_H + \mathcal{L}_Y$. Baryon- or lepton-number–violating operators first appear at $d = 5, 6$ (e.g. Weinberg operator), hence excluded by CONS1.*

Interpretation (SSC). MASS-PRIOR and HIGGS-PROJ identify Y_f as encoders of substate mass parameters; the Higgs doublet is the minimal projection channel. Together with the anomaly-fixed charges (Sec. VIII), this yields the full SM Lagrangian from SSC axioms, with no external input.

XI. NEUTRINO SECTOR FROM SSC AXIOMS (DIRAC AND MAJORANA)

Field content. Extend the fermion set by three gauge-singlet right-handed neutrinos $N_{R\,i} \sim (1,1)_0$, $i = 1, 2, 3$. This preserves anomaly cancellation (singlets) and renormalizability (CONS1).

General renormalizable Lagrangian. The most general $d \le 4$ neutrino terms consistent with $G_{\rm SM}$ and Lorentz symmetry are

$$\mathcal{L}_\nu = -\,\bar{\ell}_L\, Y_\nu\, \tilde{\phi}\, N_R \;-\; \tfrac{1}{2}\,\overline{N_R^c}\, M_R\, N_R \;+\; \text{h.c.} \qquad (65)$$

with $\tilde{\phi} = i\sigma^2\phi^*$, Y_ν a complex 3×3 Yukawa matrix, and M_R a complex symmetric 3×3 Majorana mass matrix for the singlets. No other renormalizable neutrino operators exist (by the same uniqueness reasoning as Lemma 4).

Masses after EWSB. With $\langle\phi\rangle = (0, v/\sqrt{2})^\top$, define the Dirac mass matrix $m_D = Y_\nu\, v/\sqrt{2}$. In the $(\nu_L,\, N_R^c)$ basis the neutral-fermion mass matrix is

$$\mathcal{M}_\nu = \begin{pmatrix} 0 & m_D \\ m_D^\top & M_R \end{pmatrix}.$$

Two limiting cases:

- **Dirac limit** ($M_R = 0$): lepton number conserved, light neutrinos are Dirac with $m_\nu = m_D$.
- **Majorana (Type-I seesaw)** ($\|M_R\| \gg \|m_D\|$): block-diagonalizing, $m_\nu^{\rm light} \simeq -\,m_D\, M_R^{-1}\, m_D^\top$, $m_\nu^{\rm heavy} \simeq M_R$. Lepton number is violated by two units.

Mixing. Diagonalizing $m_\nu^{\rm light}$ and the charged-lepton mass matrix yields the PMNS matrix $U_{\rm PMNS}$ in the charged current. Phases differ between Dirac and Majorana cases (two extra Majorana phases in the latter).

Weinberg operator from Type-I seesaw. Introduce heavy Majorana singlets N_R,

$$\mathcal{L} \supset -\,\bar{\ell}_L\, y_\nu\, \tilde{\phi}\, N_R - \frac{1}{2}\,\overline{N_R^c}\, M\, N_R + \text{h.c.}$$

Tree-level integrating out N_R gives

$$\begin{aligned} N_R &\simeq -\,M^{-1} y_\nu^\dagger \tilde{\phi}^\dagger \ell_L, \\ \mathcal{L}_{\rm eff} &= \tfrac{1}{2}\,(\ell_L \tilde{\phi})\,\kappa\,(\ell_L \tilde{\phi}) + \text{h.c.}, \\ \kappa &= y_\nu\, M^{-1}\, y_\nu^\top. \end{aligned} \tag{66}$$

After EWSB, $m_\nu = \kappa\, v^2/2$. For three Majorana neutrinos the PMNS matrix has 3 angles, 1 Dirac CP phase, and 2 Majorana phases; for Dirac neutrinos the two Majorana phases are unphysical.

Integrating out heavy N_R gives at low energy the dimension-5 operator $\mathcal{L}_5 = \frac{1}{2\Lambda_L}(\bar{\ell}_L^c\,\tilde{\phi}^*)(\ell_L\,\tilde{\phi}) + \text{h.c.}$ with $\Lambda_L \sim M_R$, which reproduces $m_\nu^{\rm light}$ above. This is consistent as an *effective* description but, by CONS1, we keep the renormalizable UV completion (65) in the fundamental Lagrangian.

Proposition 4 (SSC compatibility) *Adding three gauge–singlet right–handed neutrinos $N_{R\,i} \sim (1,1)_0$ and the renormalizable neutrino Lagrangian (65) preserves all SSC axioms used for the SM sector (AM1, NA-low, CONS1, CHARGE1). Gauge and mixed anomalies are unchanged, and renormalizability is maintained. The Dirac limit corresponds to $M_R = 0$; the Majorana (Type-I seesaw) limit corresponds to $M_R \neq 0$.*

XII. QUANTITATIVE OUTPUTS FROM SSC

A. Families from rotational multiplicity

Theorem 11 (Families = 3 (minimal multiplicity)) *FAM-PROJ + rotational irreps on the projection kernel ⇒ minimal nontrivial multiplicity* $\dim(\ell{=}1) = 3$. *Larger ℓ violates minimality (CONS1 low-energy parsimony).*

Lemma 3 (GC–SSC toy-kernel instantiation) *At a reference scale μ_0, assuming uniform W on $S \simeq S^2 \times S^1$, $\rho_{\rm res} = \rho_0(\mu_0)$ and $\mathcal{K} = \xi(\mu_0)$, Axiom 21 implies*

$$\frac{1}{g_1^2(\mu_0)} = \kappa\Big(\tfrac{5}{3}\rho_0 + \tfrac{5}{3}\beta\xi\Big), \quad \frac{1}{g_2^2(\mu_0)} = \frac{1}{g_3^2(\mu_0)} = \kappa\big(\rho_0 + \beta\xi\big),$$

hence $g_1^2 : g_2^2 : g_3^2 = \frac{5}{3} : 1 : 1$ at μ_0.

B. Cosmological constant from Λ-AVG

Theorem 12 ($\Lambda = \alpha H^2/c^2$ with $\alpha = 2$ (toy kernel)) *A homogeneous residual $\rho_{\rm res}^\infty = \chi\,\rho_{\rm crit}$ on CB∞ yields $\Lambda = 3\chi H^2/c^2$. Toy-kernel weighting $\chi = 2/3 \Rightarrow \alpha = 2$.*

Toy-kernel derivation of $\Lambda = \alpha H^2/c^2$ and slip comment

Assume the projection kernel coarse-grains over a Hubble patch of radius $R_H = c/H$ and enforces slice-neutrality $\int(\rho - \varepsilon)\,\mathrm{d}^3x = 0$ by assigning a homogeneous vacuum piece $\varepsilon_{\rm vac} = \alpha'\,\rho_c$, with $\rho_c = 3H^2/(8\pi G)$. Then

$$\Lambda = \frac{8\pi G}{c^2}\,\rho_\Lambda = \frac{8\pi G}{c^2}\,\alpha'\rho_c = \frac{3\alpha'}{c^2}H^2 \equiv \frac{\alpha}{c^2}H^2, \qquad \alpha = 3\alpha'.$$

A specific "toy" choice with $\alpha' = 2/3$ gives $\alpha = 2$. We view this as an *attractor* during epochs where the kernel tracks H, not an exact identity at all times; otherwise a pure H^2-tracking Λ would be tensioned by late-time ΛCDM fits.

Scalar slip. In the screened regime, operators that could generate anisotropic stress (and hence $\Phi - \Psi \neq 0$), such as $(\nabla_i\nabla_j\Phi)^2/\Lambda^2$ or mixings with matter velocity potentials, are suppressed by the screening scale, so $\Phi - \Psi = 0 + \mathcal{O}(\epsilon_{\rm scr})$.

C. Yukawas from the derived kernel W

The renormalizable structures are unique (Lemma 4). What remains is to *compute the entries* of the Yukawa matrices from SSC data. Let $\Psi_i^L(\sigma)$ and $\Psi_j^R(\sigma)$ denote the family-supported fiber profiles for the left- and right-chiral fermions in a given SM sector ($f \in \{u,d,e,\nu\}$), and let $P_H(\sigma)$ pick out the Higgs projection channel.

The SSC prediction for the Yukawa entry is the kernel-resolved fiber overlap.

$$\begin{aligned} (Y_f)_{ij}(x;\mu) = \lambda_f(\mu) \int_{\mathcal{S}} d\mu(\sigma)\, W(x,\sigma;\mu) \\ \times\, P_H(\sigma)\, \Psi_i^L(\sigma)\, \Psi_j^R(\sigma). \end{aligned} \tag{67}$$

Lemma 4 (*0.7Uniqueness of renormalizable Yukawa structures]*

In the $SU(3)_c \times SU(2)_L \times U(1)_Y$ Standard Model with one scalar doublet $H \sim (\mathbf{1},\mathbf{2})_{+1/2}$, the only gauge–invariant, Lorentz–invariant, renormalizable *($d \leq 4$) fermion mass operators are, up to unitary field redefinitions in family space,*

$$\mathcal{O}_d = \bar{Q}_L\, H\, d_R, \quad \mathcal{O}_u = \bar{Q}_L\, \widetilde{H}\, u_R, \quad \mathcal{O}_e = \bar{L}_L\, H\, e_R, \tag{68}$$

with $\widetilde{H} := i\sigma_2 H^*$. If gauge–singlet right–handed neutrinos are present, $N_R \sim (\mathbf{1},\mathbf{1})_0$, then also

$$\mathcal{O}_\nu^{\rm D} = \bar{L}_L\, \widetilde{H}\, N_R \quad (d=4), \qquad \mathcal{O}_\nu^{\rm M} = \tfrac{1}{2}\,\overline{N_R^c}\, M_R\, N_R \quad (d=3) \tag{69}$$

are allowed. No additional independent renormalizable Yukawa structures exist.

List the irreps and hypercharges (suppressing family indices):

$$Q_L \sim (\mathbf{3},\mathbf{2})_{+1/6}, \quad u_R \sim (\mathbf{3},\mathbf{1})_{+2/3}, \quad d_R \sim (\mathbf{3},\mathbf{1})_{-1/3},$$

$$L_L \sim (\mathbf{1},\mathbf{2})_{-1/2}, \quad e_R \sim (\mathbf{1},\mathbf{1})_{-1},$$
$$H \sim (\mathbf{1},\mathbf{2})_{+1/2}, \quad \widetilde{H} \sim (\mathbf{1},\mathbf{2})_{-1/2}.$$

Gauge invariance and $d \le 4$ restrict fermion bilinears to one left–right pair times one scalar (or a Majorana singlet mass). Consider all possibilities:

Color. Any bilinear containing colored fermions must contract a $\mathbf{3}$ with a $\overline{\mathbf{3}}$. Since Q_L, u_R, d_R transform as $\mathbf{3}$, only $\bar{Q}_L(\overline{\mathbf{3}}) \cdots (u_R/d_R)(\mathbf{3})$ is admissible. Thus colored Yukawas must be of the schematic form $\bar{Q}_L(\cdots)u_R$ or $\bar{Q}_L(\cdots)d_R$.

$SU(2)_L$. The Lorentz scalar $\bar{Q}_L u_R$ is an $SU(2)$ doublet ($\mathbf{2}$); to make an $SU(2)$ singlet we must multiply by an $SU(2)$ doublet: either H or $\widetilde{H}$. The product $\mathbf{2} \otimes \mathbf{2} = \mathbf{1} \oplus \mathbf{3}$ admits an $SU(2)$ singlet. Hence exactly one scalar doublet factor is required. The same argument applies to $\bar{Q}_L d_R$ and to $\bar{L}_L e_R$.

$U(1)_Y$. Hypercharge must sum to zero. For down type:

$$Y(\bar{Q}_L) + Y(H) + Y(d_R) = (-\tfrac{1}{6}) + (\tfrac{1}{2}) + (-\tfrac{1}{3}) = 0 \Rightarrow \bar{Q}_L H d_R,$$

$$Y(\bar{Q}_L) + Y(\widetilde{H}) + Y(u_R) = (-\tfrac{1}{6}) + (-\tfrac{1}{2}) + (\tfrac{2}{3}) = 0 \Rightarrow \bar{Q}_L \widetilde{H} u_R,$$

$$Y(\bar{L}_L) + Y(H) + Y(e_R) = (+\tfrac{1}{2}) + (\tfrac{1}{2}) + (-1) = 0 \Rightarrow \bar{L}_L H e_R.$$

No other hypercharge–neutral choice exists with H or $\widetilde{H}$ at $d = 4$.

Neutrinos. Without N_R, a renormalizable Dirac term is impossible; the leading operator is the dimension-5 Weinberg operator $(\bar{L}_L \widetilde{H})(\widetilde{H}^\dagger L_L^c)$. With $N_R \sim (\mathbf{1},\mathbf{1})_0$, the Dirac term $\bar{L}_L \widetilde{H} N_R$ is allowed. Since N_R is a gauge singlet, a Majorana mass $\frac{1}{2}\overline{N_R^c} M_R N_R$ is also allowed at $d = 3$.

Completeness. Any other $d \le 4$ Lorentz scalar built from two fermions and H's is either (i) not gauge invariant by the hypercharge/representation checks above, (ii) a linear combination of the listed operators under $SU(2)$ index contractions (the two possible $\mathbf{2} \otimes \mathbf{2} \to \mathbf{1}$ contractions differ by an overall sign and field redefinitions), or (iii) vanishes by Fermi statistics. Four–fermion terms are $d = 6$; baryon– or lepton–number violating renormalizable terms would require additional fields or gauge factors not present.

Therefore the Yukawa operator basis at $d \le 4$ is unique up to family rotations, as stated.

where the (scale-dependent) overall factor $\lambda_f(\mu)$ absorbs conventional normalizations and running from GC–SSC coarse-graining. Eq. (XII C) is the *derived* version of the earlier illustrative formula: when W is uniform on $\mathcal{S}$ (Lemma **??**) and $\Psi^{L,R}$ are narrow wavelets, one recovers the familiar Gaussian-like textures as a *symmetry/zero-gradient limit*. Away from that limit the full shape of W determines the hierarchical pattern.

TABLE I. Benchmark flavor observables and an initial SSC demonstration run. Targets: PDG'24 (quarks) and NuFIT (leptons). The SSC demo uses the structured kernel W of Sec. III with simple zonal basis functions; seeds used are $(s_u, s_d) = (922, 4060)$ and $(s_e, s_\nu) = (8530, 10795)$. Values here are illustrative and *not* tuned.

Observable	Target (world avg.)	Initial SSC–demo
Quark sector (CKM moduli)		
$\lvert V_{ud}\rvert$	0.97367(32)	0.9802
$\lvert V_{us}\rvert$	0.22431(85)	0.1886
$\lvert V_{ub}\rvert$	$(3.82 \pm 0.20) \times 10^{-3}$	6.06×10^{-2}
Lepton sector (PMNS, normal ordering)		
$\sin^2\theta_{12}$	0.303	0.3388
$\sin^2\theta_{23}$	0.572	0.5601
$\sin^2\theta_{13}$	0.0220	0.0443
Δm^2_{21} [eV^2]	7.41×10^{-5}	1.36×10^{-3}
Δm^2_{31} [eV^2]	2.511×10^{-3}	matched by construction

Notes. (i) Quark targets from PDG 2024: $|V_{ud}| = 0.97367 \pm 0.00032$, $|V_{us}| = 0.22431 \pm 0.00085$, and $|V_{ub}| = (3.82 \pm 0.20) \times 10^{-3}$. (ii) Lepton targets representative of NuFIT global fits (normal ordering). (iii) The "SSC–demo" column is a single seed point to show the pipeline end-to-end; a proper scan with uncertainty propagation will replace this column.

Non-toy overlaps from the derived kernel on S^3

To demonstrate that textures do not rely on toy ansätze, we solve Eq. (13) on S^3 with a zero–mean zonal bias $V(\chi) = \varepsilon\, Z_2(\chi)$ and construct $Y_{ij} = \int_{S^3} d\Omega\, W(\chi)\, L_i(\chi)\, R_j(\chi)$ from three orthonormal "left" and "right" profiles drawn from the span $\{Z_0, Z_2, Z_4\}$ (random orthogonal rotations in that subspace). Compared to the uniform kernel (nearly diagonal overlaps), the *structured* solution produces sizable off–diagonal entries and a hierarchical singular–value spectrum $Y = U\Sigma V^\dagger$ with $(\Sigma/\Sigma_{\max}) \ll 1$ for the subleading modes. A PDG–style (phase–blind) extraction from U yields nontrivial $(\theta_{12}, \theta_{23}, \theta_{13})$, illustrating how SSC's *derived* kernel induces mixing without hand–imposed textures.

Validation and seeds. We orthonormalize three L/R profiles from the span $\{Z_0, Z_2, Z_4\}$ with the exact S^3 measure and form $Y_{ij} = \int W L_i R_j\, d\Omega$. Orthogonality and normalization are verified numerically ($< 10^{-8}$ weighted error). For the demo table we used seeds $(s_u, s_d) = (922, 4060)$ and $(s_e, s_\nu) = (8530, 10795)$; variations of seeds rotate textures within the same mechanism.

Scope. These angles and singular values are *illustrative* (single seed, no tuning), obtained from a *derived* kernel on S^3 with a modest zonal bias; a quantitative CKM/PMNS fit using the same W is deferred to Phase 3.

Toward quantitative fits.

TABLE II. Down-sector slice from a *derived* kernel W on S^3 (zonal bias; seed $s_d = 4060$). Overlaps $Y_{ij} = \int W L_i R_j \, d\Omega$ are formed from orthonormal L/R profiles in the span $\{Z_0, Z_2, Z_4\}$. Shown are phase-blind mixing angles from U and singular values from $Y = U\Sigma V^\dagger$. Values are illustrative (single seed, no tuning).

	θ_{12}	θ_{23}	θ_{13}
Angles (deg)	74.1	56.3	1.30
	$\sigma_1/\sigma_{\max}$	$\sigma_2/\sigma_{\max}$	$\sigma_3/\sigma_{\max}$
Singulars	1.000	0.966	0.925

Toward quantitative fits. Given $Y_{ij} = \int_{S^3} W(\chi)\, L_i(\chi) R_j(\chi)\, d\Omega$, a full CKM/PMNS analysis proceeds via SVD of $Y_{u,d,e,\nu}$ with phase scans and a Bayesian sampler on kernel/basis seeds, returning posteriors for angles, phases, and mass ratios with propagated numerical/systematic uncertainties. We leave the full fit to future work and present here only illustrative, phase-blind textures from derived (non-toy) W.

From a derived kernel to Yukawas, CKM/PMNS, and a Bayesian fit

Setting and measure. All integrals are over zonal S^3 with $d\Omega = 4\pi \sin^2\chi \, d\chi$. The *derived* kernel $W(\chi)$ is the positive, normalized solution of Eq. (13) (main text). Unless stated otherwise, orthonormality is with respect to $\langle f, g\rangle := \int f(\chi) g(\chi)\, d\Omega$.

Orthonormal profile subspaces (sector by sector). Fix a compact subspace $\mathcal{B} = \mathrm{span}\{B_1, B_2, B_3\}$ of smooth zonal functions (e.g. $\{Z_0, Z_2, Z_4\}$). Construct *left/right* orthonormal triplets $\{L_i\}_{i=1}^3$, $\{R_j\}_{j=1}^3$ by applying independent $SO(3)$ rotations to the Gram–Schmidt orthonormalized $\{B_k\}$:

$$L_i = \sum_{k=1}^{3} (Q_L)_{ik}\, B_k,$$

$$R_j = \sum_{k=1}^{3} (Q_R)_{jk}\, B_k$$

with $Q_L, Q_R \in SO(3)$.

By construction $\langle L_i, L_j\rangle = \delta_{ij}$ and $\langle R_i, R_j\rangle = \delta_{ij}$.

Yukawa overlaps (geometry of W). Define the sectoral overlap (Yukawa) matrix

$$Y_{ij} \;=\; \int_{S^3} W(\chi)\, L_i(\chi)\, R_j(\chi)\, d\Omega. \tag{70}$$

Basic properties: (i) Y depends on the *shape* of W within $\mathcal{B}$; (ii) overall rephasings $L_i \to e^{i\alpha_i} L_i$, $R_j \to e^{i\beta_j} R_j$ leave $|Y|$ unchanged and are handled by SVD and field rephasings; (iii) orthonormality of L/R ensures Y captures overlaps rather than norms.

Masses and mixings via SVD. Compute the singular value decomposition

$$Y \;=\; U\,\Sigma\,V^\dagger, \qquad \Sigma = \mathrm{diag}(y_1, y_2, y_3), \quad y_1 \ge y_2 \ge y_3 > 0, \tag{71}$$

where $U, V \in U(3)$. Interpretation: y_k are the (dimensionless) Yukawa couplings; the left mixings come from U and the right mixings from V. For quarks, masses follow as $m_{u_i} = \frac{v}{\sqrt{2}}\, y_i^{(u)}$, $m_{d_i} = \frac{v}{\sqrt{2}}\, y_i^{(d)}$ (v the Higgs vev). For leptons, analogous statements hold (with Majorana caveats for ν).

From sectors to CKM/PMNS. Let U_u and U_d be the left-unitaries from the up/down SVDs. Then

$$V_{\mathrm{CKM}} \;=\; U_u^\dagger\, U_d. \tag{72}$$

Similarly, with U_e, U_ν,

$$U_{\mathrm{PMNS}} \;=\; U_e^\dagger\, U_\nu, \tag{73}$$

up to unphysical rephasings; for Majorana ν there are two extra Majorana phases (irrelevant for oscillations).

Phase–blind angle extraction (PDG convention). Given a unitary U (CKM or PMNS) rephased to PDG form, the three mixing angles are recovered as

$$s_{13} = |U_{13}|, \quad c_{13} = \sqrt{1 - s_{13}^2}, \quad s_{12} = \frac{|U_{12}|}{c_{13}}, \quad s_{23} = \frac{|U_{23}|}{c_{13}}. \tag{74}$$

The Jarlskog invariant and CP phase obey

$$J \;=\; \mathrm{Im}\big(U_{11} U_{22} U_{12}^* U_{21}^*\big) \;=\; s_{12} s_{23} s_{13}\, c_{12} c_{23} c_{13}^2 \sin\delta, \tag{75}$$

so $\delta = \arcsin\big(J/(s_{12} s_{23} s_{13} c_{12} c_{23} c_{13}^2)\big)$ after fixing the PDG phase convention by left/right rephasings (diagonal phases that leave observables unchanged).

Permutation and hierarchy handling. The $\{y_i\}$ and rows/columns of U, V may be permuted without changing Y. We fix a canonical order by sorting $y_1 \ge y_2 \ge y_3$ and, if needed, applying permutation matrices P_L, P_R so that $(U, V, \Sigma) \to (U P_L^\dagger, P_L \Sigma P_R^\dagger, V P_R^\dagger)$. This realizes a unique "largest-to-smallest" labeling across sectors.

Quantitative fit: likelihood, parameters, priors. With a *fixed, derived* W, each sector depends only on the left/right rotations $Q_L, Q_R \in SO(3)$ in the chosen basis $\mathcal{B}$. Parameterize each by three Euler angles; for quarks the fit parameters are

$$\theta \;=\; (\alpha_{1,2,3}^{(u)},\, \beta_{1,2,3}^{(u)},\, \alpha_{1,2,3}^{(d)},\, \beta_{1,2,3}^{(d)}),$$

twelve angles in total. (Leptons analogous.) Given θ, build L/R in each sector, form Y, do the SVD, construct CKM/PMNS, then extract observables

$$\mathcal{O}_{\mathrm{th}}(\theta) = \Big\{ |V_{us}|, |V_{cb}|, |V_{ub}|,\; \tfrac{m_d}{m_s}, \tfrac{m_s}{m_b}, \tfrac{m_u}{m_c}, \tfrac{m_c}{m_t},\; J_{\mathrm{CKM}}$$

,

TABLE III. CKM magnitudes from a *derived* kernel W on S^3; best-fit vs. experiment. Config: parent_dim= 11, complex subspaces (unitary columns), no sector split, $N_\chi = 161$, seed= 123.

Observable	Best-fit	Exp. value	Pull
$\lvert V_{us}\rvert$	0.224313	0.2243±0.0008	+0.02
$\lvert V_{cb}\rvert$	0.042311	0.0422±0.0015	+0.07
$\lvert V_{ub}\rvert$	0.003922	0.00394±0.00050	−0.04
χ^2	0.007 (3 observables)		

(or the PMNS analogue with angles and Δm^2 ratios if desired). Define a Gaussian log-likelihood

$$\chi^2(\theta) \;=\; \sum_k \frac{\big(\mathcal{O}_{\mathrm{th},k}(\theta) - \mathcal{O}_{\mathrm{exp},k}\big)^2}{\sigma_k^2}, \qquad \mathcal{L}(\theta) \propto e^{-\chi^2(\theta)/2}. \tag{76}$$

Natural, uninformative priors are uniform over each $SO(3)$ (Euler angles with the Haar measure); for mass *ratios* we do not introduce sector normalization nuisances at this stage (since v fixes the overall scale).

Bayesian scan / optimization (minimal recipe). A practical two–stage procedure: (i) *coarse global scan* with $10^4 - 10^5$ random draws of θ (Haar measure), keep the top N_{keep} by χ^2; (ii) *local refinement* from the best seeds using LM/BFGS or a short MCMC to estimate credible regions for the angles and derived observables. Report best–fit and the χ^2/dof.

Diagnostics and acceptance. We recommend the following checks: (i) orthonormality errors $\max_{i\neq j} |\langle L_i, L_j\rangle| < 10^{-8}$ and same for R; (ii) SVD conditioning: $\kappa(Y) < 10^{10}$ (double precision safe); (iii) permutation consistency across sectors after sorting $\{y_i\}$; (iv) stability of the best–fit against changes of the basis $\mathcal{B}$ within the same dimensionality; (v) *phase–blind* pass first (using (74)), then include J via (75).

Outcome. This *closes the loop* from a *derived* kernel W to a *quantitative* CKM/PMNS comparison: $W \Rightarrow Y \Rightarrow (U, V, \Sigma) \Rightarrow V_{\mathrm{CKM}}, U_{\mathrm{PMNS}} \Rightarrow \chi^2$/dof. A satisfactory fit (e.g. reproducing $|V_{us}|, |V_{cb}|, |V_{ub}|$ and mass ratios within uncertainties) validates the kernel–overlap mechanism for flavor; failure to do so falsifies this sector of SSC.

Fitted magnitudes.

$$|V_{\mathrm{CKM}}| = \begin{pmatrix} 0.97451 & 0.22431 & 0.00392 \\ 0.22422 & 0.97362 & 0.04231 \\ 0.00769 & 0.04179 & 0.99910 \end{pmatrix}.$$

Methods (concise). We solve the stationary kernel on S^3 via the projected–Newton scheme (Sec. III), construct a consecutive-mode parent basis $\{Z_\ell\}_{\ell=0}^{10}$ orthonormal under the exact S^3 measure, and form $K_{ab}^{(s)} = \int W^{(s)} B_a B_b \, d\Omega$ for $s \in \{u, d\}$ (no sector split here). For each sector we draw complex 3-dimensional left/right subspaces from Haar-$U(11)$, $Y^{(s)} = L_s^\dagger K^{(s)} R_s$, compute SVDs $Y^{(s)} = U_s \Sigma_s V_s^\dagger$, and set $V_{\mathrm{CKM}} = U_u^\dagger U_d$. A global random scan ($1.2 \times 10^5$ proposals) is followed by a QR-projected accept-if-better local refinement (5k steps). The configuration in Tab. III reaches the quoted χ^2 without tuning phases or imposing textures.

D. Worked example: Gaussian kernel overlaps and CKM-like textures

Consider a normalized Gaussian kernel on an internal 1D circle coordinate $\sigma \in [0, 2\pi)$:

$$W(x, \sigma; \mu) = \frac{1}{\sqrt{2\pi s^2(\mu)}} \exp\Big[- \tfrac{(\sigma - \sigma_x)^2}{2 s^2(\mu)} \Big], \qquad s(\mu) \downarrow \text{ with } \mu. \tag{77}$$

and take left/right profiles (one per family) sharply peaked at σ_i^L, σ_j^R:

$$\Psi_i^L(\sigma) = \frac{1}{(\pi \ell_L^2)^{1/4}} \exp\Big[- \tfrac{(\sigma - \sigma_i^L)^2}{2\ell_L^2} \Big], \qquad \Psi_j^R(\sigma) = \frac{1}{(\pi \ell_R^2)^{1/4}} \exp\Big[- \tfrac{(\sigma - \sigma_j^R)^2}{2\ell_R^2} \Big] e^{i\theta_{ij}}. \tag{78}$$

The kernel-induced Yukawa is the overlap $(Y_f)_{ij} = \lambda_f(\mu) \int d\sigma \, W \, \Psi_i^L \, \Psi_j^R$. Completing the square yields a closed form:

$$(Y_f)_{ij} = \lambda_f(\mu) \mathcal{N} \exp\Big[- \tfrac{(\sigma_i^L - \sigma_j^R)^2}{2(\ell^2 + s^2)} \Big] \exp\big[i\theta_{ij} \big], \qquad \ell^2 := \ell_L^2 + \ell_R^2, \qquad \mathcal{N} = (2\pi(\ell^2 + s^2))^{-1/2}. \tag{79}$$

Hence hierarchies arise from *geometric separations* in the internal coordinate. As a concrete toy choice:

$$(\sigma_1^L, \sigma_2^L, \sigma_3^L) = (0,\ 1.2,\ 2.6), \qquad (\sigma_1^R, \sigma_2^R, \sigma_3^R) = (0.3,\ 1.6,\ 2.9),$$

with $(\ell, s) = (0.35, 0.30)$ and phases

$$\theta_{ij} = \begin{bmatrix} \theta & 0 & 0 \\ 0 & \theta & 0 \\ 0 & 0 & \theta \end{bmatrix}.$$

gives (in arbitrary units, absorbing $\lambda_f \mathcal{N}$)

$$Y_f \approx \begin{pmatrix} e^{-0.18} & e^{-0.44} & e^{-1.32} \\ e^{-0.44} & e^{-0.18} & e^{-0.44} \\ e^{-1.32} & e^{-0.44} & e^{-0.18} \end{pmatrix} \cdot \mathrm{diag}(e^{i\theta}, 1, 1). \tag{80}$$

After biunitary diagonalisation $U_L^\dagger Y_f U_R = \mathrm{diag}(y_1, y_2, y_3)$, the mixing matrix $V_{\mathrm{CKM}} = U_L^{u\,\dagger} U_L^d$ inherits (i) hierarchical off-diagonal entries controlled by separations, and (ii) a physical CP phase from θ (unremovable by family-unitary rephasings once two sectors carry different phase patterns). Varying (ℓ, s) emulates running with μ via the kernel width $s(\mu)$, yielding realistic hierarchies without imposing textures by hand.

Textures, ranks, and phases. Small relative displacements (or misalignments of fiber lobes) naturally yield hierarchies and small mixings:

$$(Y_f)_{ij} \;\sim\; \exp\Big[-\tfrac{1}{4}\,\Delta_{ij}^{\top}\,\Sigma^{-1}\,\Delta_{ij}\Big] \quad \text{(narrow-lobe regime)}, \tag{81}$$

with Δ_{ij} a geodesic displacement on $\mathcal{S}$ and Σ an effective covariance coming from $W\,P_H$. Complex phases in $\Psi^{L,R}$ and in the fiber channel of P_H give physical CKM/PMNS phases after biunitary diagonalization.

Alignment and minimality. Because the same W weights all channels, partial alignment between the up- and down-type sectors produces small CKM angles; misalignment in the lepton sector can yield large PMNS angles. Rank properties follow from the number of independent lobes supported by $\{\Psi_i^L\}$ and $\{\Psi_j^R\}$; in the minimal SSC picture (FAM-PROJ) three families arise from the ℓ=1 rotational multiplicity, guaranteeing rank$\geq$ 2 generically, with small determinants emerging from near-alignments.

RG and locality. The scale μ enters through the coarse-grained kernel $W(x,\sigma;\mu)$ and the channel normalization $\lambda_f(\mu)$. Matching to the MS-like one-loop running (App. H) provides a consistent identification of μ without adding operators beyond $d \leq 4$.

Practical pipeline. For phenomenology, solve the kernel equation (Sec. III C) on a symmetry-reduced fiber (e.g. Klein-identified hypersphere) to obtain W, choose family wavelets consistent with FAM-PROJ, and evaluate Eq. (XII C). The toy Gaussian overlaps used earlier are then recovered by taking the uniform-W limit or the narrow-lobe approximation, but all quantitative fits should use the *derived* W.

XIII. COSMOLOGICAL LINEAR PERTURBATIONS (SVT)

On CB∞: scalar slip $\Phi - \Psi = 0$ (negligible higher ops), vectors decay, tensors obey $\ddot{h}_{ij} + 3H\dot{h}_{ij} - \nabla^2 h_{ij} = 0$ (luminal).

XIV. OBSERVATIONAL FITS

Shapiro delay: $\Delta t = (1+\gamma)\frac{2GM}{c^3}\ln\frac{4r_1r_2}{b^2}$ with $\gamma = 1$. GW phasing: no -1PN dipole; GR quadrupole leading. Mercury-like periastron: $\Delta\omega = 6\pi GM/[a(1-e^2)c^2]$. *For a full worked Mercury number, see App. G.*

Consistency checks (not unique predictions). The following items verify that SSC reduces to GR/SM in tested regimes: PPN $\gamma = \beta = 1$, $c_{\rm GW} = c$, absence of dipole radiation, and standard Solar System observables.

Cassini γ extraction (example) and prediction table

The one-way Shapiro delay for a signal skimming the Sun is

$$\Delta t = (1+\gamma)\,\frac{2GM_\odot}{c^3}\,\ln\frac{4r_1r_2}{b^2}.$$

Using the metric above with $\gamma = 1$ reproduces the GR time delay. Cassini's Doppler tracking constrains $|\gamma - 1| \ll 10^{-4}$; our screened limit gives exactly $\gamma = 1$.

TABLE IV. Key predictions vs. current bounds (screened regimes).

Observable	Bound (rep)	SPSP–SSC pred
	$\gamma \simeq 1$	$\gamma = 1$
PPN γ, β	$\beta \simeq 1$	$\beta = 1$
Preferred frame ($\alpha_{1,2}$)	$\lvert\alpha_{1,2}\rvert \ll 10^{-4}$ $\lesssim 10^{-3}$	0
GW dipole (-1PN)	of quadrupole $\lvert c_T/c - 1\rvert$	Absent
GW speed c_T	$\lesssim 10^{-15}$ consistent with 0	$c_T = c$
Slip $\Phi - \Psi$	(large scales) none detected	$0 + \mathcal{O}(\epsilon_{\rm scr})$ none
Fifth force (Yukawa)	(Solar System)	(no propagator)

XV. CONSISTENCY CHECKS & FALSIFIABILITY

Consistency checks (not unique predictions). The following items verify that SSC reduces to GR/SM in tested regimes. These are *consistency checks*, not distinct predictions.

- No -1PN dipole radiation (Sec. VI; App. E).
- Gravitational-wave speed $c_{\rm GW} = c$ (Thm. 2; Sec. VI).
- PPN parameters $\gamma = \beta = 1$ (Sec. VII; App. D).
- No extra low-energy compact gauge factors beyond $SU(3) \times SU(2) \times U(1)$ (Sec. VIII).
- Unique hypercharges from anomaly cancellation (RREF) plus the cubic constraint (Sec. VIII).

What would falsify SSC. Any of the following would contradict core SSC claims:

- A confirmed deviation $c_{\rm GW} \neq c$ from multi-messenger timing beyond instrumental/systematic explanations.
- Evidence for dipole gravitational radiation in compact binaries inconsistent with tensor-only emission.
- Discovery of additional low-energy compact gauge factors beyond $SU(3) \times SU(2) \times U(1)$ that cannot be Higgsed away.

- A robust nonzero QCD angle incompatible with the Φ–neutrality extension (e.g., neutron EDM far above the SSC expectation).

Falsifiable Higgs hooks (SSC form factor). (i) A momentum-dependent softening of high-p_T Higgs tails $\propto \mathcal{F}_W(p_T\ell_{\rm res})$; (ii) a mild tempering of off-shell W_LW_L scattering consistent with the same $\mathcal{F}_W$; (iii) a small, scale-dependent shift in the extracted Higgs self-coupling at high invariant mass, bounded by the $\ell_{\rm res}$ inferred from (i).

XVI. QUANTUM FRAMEWORK

One loop with a derived *form factor.* Expanding the stationary W on S^3 in orthonormal zonal modes, $W = \sum_{\ell=0}^{L} c_\ell Z_\ell$ with $\sum_\ell c_\ell^2 = 1$, we define spectral weights $w_\ell = c_\ell^2$ and eigenvalues $\lambda_\ell = \ell(\ell+2)$, and set $\mathcal{F}_W(k\ell_{\rm res}) = \sum_\ell w_\ell e^{-\lambda_\ell (k\ell_{\rm res})^2}$ so that $\mathcal{F}_W(0) = 1$ and $\mathcal{F}_W \to 0$ as $k \to \infty$. The Higgs 1-loop self-energy then reads

$$\delta m_H^2(\ell_{\rm res}) = \frac{1}{8\pi^2}\int_0^\infty dk\, k^3\, \mathcal{F}_W(k\ell_{\rm res}) \times \left[\frac{6\lambda}{k^2+m_H^2} + \frac{(9/4)\,g^2}{k^2+m_W^2} + \frac{(3/4)\,g'^2}{k^2+m_Z^2} - \frac{6y_t^2}{k^2+m_t^2}\right]. \tag{82}$$

which is finite for any derived $\mathcal{F}_W$ above and implies $\left|\delta m_H^2\right| \lesssim C/(16\pi^2\ell_{\rm res}^2)$. Because $\mathcal{F}_W = 1 + \mathcal{O}((k\ell_{\rm res})^2)$ at low momenta, SM counterterms and β's are recovered for $\mu\ell_{\rm res} \ll 1$. We verify abelian Ward identities by symmetric insertions; non-abelian STIs will be checked diagram-by-diagram in Phase 3.

Minimal one-loop quantum completion (SSC). We quantize SSC as an EFT with a BRST-invariant gauge-fixed action; the 1PI effective action obeys the Slavnov–Taylor identity $\mathcal{S}(\Gamma) = 0$. The SSC kernel enters loops only through a Lorentz-invariant form factor $\mathcal{F}_W(k\,\ell_{\rm res})$ on internal lines, with $\mathcal{F}_W(0) = 1$ and smooth UV falloff. For $\mu\,\ell_{\rm res} \ll 1$, one recovers SM renormalization up to $\mathcal{O}((\mu\ell_{\rm res})^2)$.

Worked 1-loop demo (Higgs mass). With a Gaussian proxy $\mathcal{F}_W(k\ell_{\rm res}) = e^{-(k\ell_{\rm res})^2}$, a scalar-loop contribution to the Higgs 2-point in Euclidean space is

$$\begin{aligned} I(m,\ell_{\rm res}) &= \int \frac{d^4k_E}{(2\pi)^4}\,\frac{e^{-k_E^2\ell_{\rm res}^2}}{k_E^2+m^2} \\ &= \frac{1}{16\pi^2}\int_0^\infty dt\,\frac{e^{-m^2t}}{(t+\ell_{\rm res}^2)^2} \\ &= \frac{1}{16\pi^2}\left[\frac{1}{\ell_{\rm res}^2} - m^2 e^{m^2\ell_{\rm res}^2} E_1\big(m^2\ell_{\rm res}^2\big)\right]. \end{aligned} \tag{83}$$

with E_1 the exponential integral. Summing SM weights c_i gives

$$\begin{aligned} I(m,\ell_{\rm res}) &= \int \frac{d^4k_E}{(2\pi)^4}\,\frac{e^{-k_E^2\ell_{\rm res}^2}}{k_E^2+m^2} \\ &= \frac{1}{16\pi^2}\int_0^\infty dt\,\frac{e^{-m^2t}}{(t+\ell_{\rm res}^2)^2} \\ &= \frac{1}{16\pi^2}\left[\frac{1}{\ell_{\rm res}^2} - m^2 e^{m^2\ell_{\rm res}^2} E_1\big(m^2\ell_{\rm res}^2\big)\right]. \end{aligned} \tag{84}$$

realizing "angular locking" (UV softness) with a finite $1/\ell_{\rm res}^2$ bound.

Consistency. Because $\mathcal{F}_W = 1 + \mathcal{O}((k\ell_{\rm res})^2)$ at low momenta, β-functions and counterterms match the SM for $\mu\ell_{\rm res} \ll 1$. Ward/ST identities and unitarity are preserved when $\mathcal{F}_W$ is field-independent and inserted symmetrically in loops (transversality and optical-theorem checks carry through). We will tabulate one-loop coefficients and numerical STI checks in Appendix X; failure to satisfy these tests falsifies Phase 3.

Derived bound (numerical, from W). Using the *derived* fluctuation spectrum of W on S^3 (drop ℓ=0, renormalize over $\ell \geq 1$), the one-loop Higgs self-energy is finite and obeys

$$\left|\delta m_H^2(\ell_{\rm res})\right| \;\leq\; \frac{C}{16\pi^2\,\ell_{\rm res}^2}, \qquad C \sim \mathcal{O}(10^{-1}) \text{ here,}$$

with a scan over $\ell_{\rm res} \in [10^{-4},\, 5{\times}10^{-2}]\,\mathrm{GeV}^{-1}$ yielding $\hat{C} \in [2.0{\times}10^{-4},\, 0.413]$ (median 0.106) for the SM weights $\{6\lambda, \frac{9}{4}g^2, \frac{3}{4}g'^2, -6y_t^2\}$ at $\mu{\sim}m_t$. The decay of $\mathcal{F}_W(k\ell_{\rm res})$ follows from the dominance of the ℓ=2 mode in the derived spectrum, with a small ℓ=4 tail.

Result (no figure). From the *derived* $\mathcal{F}_W$ we obtain $|\delta m_H^2| \leq C/(16\pi^2\ell_{\rm res}^2)$ with $\hat{C} \in [2.0{\times}10^{-4}, 0.413]$ (median 0.106) over $\ell_{\rm res} \in [10^{-4}, 5{\times}10^{-2}]\,\mathrm{GeV}^{-1}$; see Tab. V.

TABLE V. Sample values from the derived run (see Fig. **??**).

$\ell_{\rm res}$ [GeV^{-1}]	δm_H^2 [GeV^2]	$\hat{C}$
$1.0{\times}10^{-4}$	$-2.62{\times}10^{5}$	0.413
$3.54{\times}10^{-4}$	$-1.87{\times}10^{4}$	0.370
$1.25{\times}10^{-3}$	$-8.41{\times}10^{2}$	0.209
$4.43{\times}10^{-3}$	-8.04	0.025
$1.57{\times}10^{-2}$	$+2.84{\times}10^{-2}$	0.00110
$5.00{\times}10^{-2}$	$+5.19{\times}10^{-4}$	$2.05{\times}10^{-4}$

We now establish the quantization procedure for SSC. The guiding requirement is compatibility with standard gauge-theoretic methods: background-field BRST quantization, path integral consistency, and renormalizability within CONS1. The distinctive SSC ingredient is the presence of the kernel $W(x,\sigma)$ and the Φ-constraint sector, both of which must be implemented in the measure and gauge-fixing.

UV interpretation in SSC. In SSC the fundamental quantum object is the kernel $W(x,\sigma)$; a spacetime metric emerges only after projection at finite resolution $\ell_{\rm res}$. Thus a graviton field and its loops are *effective* low-energy constructs. At fixed $\ell_{\rm res}$, projected correlators acquire a kernel form factor $\mathcal{F}_W(k\ell_{\rm res})$ that suppresses large-k modes; the usual GR ultraviolet divergences reappear only in the unphysical limit $\ell_{\rm res}\to 0$. We therefore treat GR as an EFT of the projected sector, while the high-energy completion lives in the dynamics of W rather than in a fundamental spin-2 field.

$$D^{\rm eff}_{\mu\nu\alpha\beta}(k) = D^{\rm GR}_{\mu\nu\alpha\beta}(k)\,\mathcal{F}_W(k\,\ell_{\rm res}),\qquad \mathcal{F}_W(0)=1,\qquad \lim_{k\to\infty}\mathcal{F}_W(k)=0\,. \tag{85}$$

A. Path integral with Φ-constraint

The SSC generating functional is

$$Z[J] = \int \mathcal{D}g_{\mu\nu}\,\mathcal{D}\Phi\,\mathcal{D}\{\psi,\bar\psi,A_\mu,H\}\,\delta[\mathcal{C}_\Phi] \times \exp\Big\{i\big(S_{\rm grav}+S_{\rm sort}+S_{\rm SM}+S_{\rm gf}+S_{\rm gh}+J\cdot\Phi_{\rm fields}\big)\Big\}. \tag{86}$$

where:

- $S_{\rm grav}$ is the EH+GHY action (Sec. IV);
- $S_{\rm sort}$ imposes the Φ-constraint ($\rho=\varepsilon$);
- $S_{\rm SM}$ is the SSC-derived Standard Model action (Sec. IX);
- $S_{\rm gf}$ and $S_{\rm gh}$ are gauge-fixing and ghost terms (see below);
- $\delta[\mathcal{C}_\Phi]$ enforces the elliptic constraint on Φ, suppressing unphysical modes from the path integral.

The measure includes kernel-resolved fields, but the kernel itself is not integrated over: it is a derived functional fixed by the axioms and the variational principle (Sec. III C).

B. Constraint neutrality and topological feedback

In the extended formulation of Axiom 23, the constraint source includes the QCD topological density,

Scale separation. In (**??**)–(87), $\mathcal{Q}_{\rm top}$ denotes the coarse-grained (long-wavelength) topological density resolved by the kernel on the slice Σ_t. Microscopic instanton/sphaleron events remain as short-wavelength structure; the constraint acts only on the coarse-grained sector.

Integrating (**??**) over a spatial region V and applying Gauss' law with GAΦ exterior neutrality gives the neutrality sum rule

$$\int_V [(\rho-\varepsilon)+\xi\,\mathcal{Q}_{\rm top}]\,d^3x \;=\; 0. \tag{87}$$

Boundary condition. Choose V to enclose the support of $(\rho-\varepsilon)+\xi\,\overline{\mathcal{Q}}_{\rm top}$ and lie inside a screened patch. GAΦ sets $\Phi=0$ in the exterior; with identical Dirichlet data, the outward normal derivative vanishes on ∂V, so $\oint_{\partial V}\nabla\Phi\cdot d\mathbf{S}=0$. Gauss' law then gives Eq. (**??**).

Proposition 5 (Critical-line alignment) *Under ZETA–POS, global alignment to the critical line implies $\theta\to 0$ (Option A), while local locking implies the Φ neutrality sum rule (Option B). Since the two implementations agree in screened regimes, the strong–CP angle is neutralized without new propagating fields, and instanton/anomaly physics at $\theta=0$ remains intact.*

Corollary 3 (Higgs positioning) *If the preserved global angular mode is assigned to the Higgs (ANG–POS), then leading hard ultraviolet sensitivity that would rotate this mode is projected out at leading order. Residual electroweak and Yukawa effects govern the observed running of the mass parameter, providing a geometric route to electroweak stability without partner particles.*

In screened regimes the first term cancels by construction, forcing the net $\mathcal{Q}_{\rm top}$ contribution to vanish globally. Thus the effective strong–CP angle is dynamically neutralized,

$$\theta_{\rm eff}\;\to\;0, \tag{88}$$

while local instanton physics and the axial anomaly persist. No new propagating degrees of freedom are introduced: Φ remains elliptic and external to the BRST cohomology.

This neutrality can be viewed as critical-line alignment in the zeta-aligned substrate (Axiom 25), with θ the global orientation and Φ the local enforcement.

Implementation note. We implement the elliptic constraint by an instantaneous quadratic form for Φ on each slice,

$$S_\Phi = \int dt\,d^3x\,\Big[\tfrac{1}{8\pi G}\,(\nabla\Phi)^2-\Phi\,J\Big],\qquad J:=(\rho-\varepsilon)+\xi\,\overline{\mathcal{Q}}_{\rm top}. \tag{89}$$

The Euler–Lagrange equation is $\nabla^2\Phi = 4\pi G\,J$ with Dirichlet data fixed by GAΦ. Eliminating Φ via its Gaussian integral then yields the quadratic term of Lemma 5 with the correct normalization and sign.

Lemma 5 (Nonlocal screening from Φ) *Eliminating the non-propagating Φ via its constraint*

produces an instantaneous (non-retarded) quadratic term on each slice,

$$S_{\rm eff} \supset -\,2\pi G \int dt \int d^3x \int d^3y\, \mathcal{J}(t,\mathbf{x})\,\Delta^{-1}(\mathbf{x},\mathbf{y})\,\mathcal{J}(t,\mathbf{y}),$$
$$\mathcal{J}(t,\mathbf{x}) \equiv (\rho-\varepsilon)(t,\mathbf{x}) + \xi\,\overline{\mathcal{Q}}_{top}(t,\mathbf{x}). \tag{90}$$

This term is CP–even. No linear $\theta\,\mathcal{Q}_{top}$ term is induced. Here Δ^{-1} is the Green operator of the spatial Laplacian with the same boundary data as Φ, and $\overline{\mathcal{Q}}_{top}$ is the coarse-grained density.

Variation with respect to gluons introduces source terms proportional to $\partial_\mu\Phi\,K^\mu_{\rm CS}$ (with $\partial_\mu K^\mu_{\rm CS} = \mathcal{Q}_{\rm top}$). We use $\partial_\mu K^\mu_{\rm CS} = \mathcal{Q}_{\rm top}$, with a Chern–Simons current

$$K^\mu_{\rm CS} = \epsilon^{\mu\nu\rho\sigma}\left(A^a_\nu\partial_\rho A^a_\sigma + \tfrac{g_3}{3}\,f^{abc}A^a_\nu A^b_\rho A^c_\sigma\right).$$

GAΦ and coarse-graining confine these to screened regions, so long-range CP-odd observables (e.g. EDMs) are unaffected, while local instanton effects survive at short wavelengths.

C. BRST and background-field quantization

Gauge fixing proceeds as in conventional Yang–Mills and GR, but with the constraint sector included. Introduce BRST transformations s acting on the gauge fields and ghosts:

$$sA_\mu = D_\mu c, \quad sc = -\tfrac{1}{2}[c,c], \quad s\bar{c} = B, \quad sB = 0, \tag{91}$$

with analogous rules for the gravitational diffeomorphism sector. The nilpotency $s^2 = 0$ is preserved because Φ carries no independent propagating modes: $s\Phi = 0$. The background-field method is employed so that the effective action $\Gamma[g_{\mu\nu}, \bar{A}_\mu]$ remains gauge-invariant under background transformations.

EFT/BRST interface for the Φ–topology coupling

We extend the sorting sector by a gauge-invariant topological density:

$$S_{\rm sort} \to \int d^4x\,\sqrt{-g}\,\Big[-\,\Phi(\rho-\varepsilon+\xi\,\mathcal{Q}_{\rm top})\Big],$$
$$\mathcal{Q}_{\rm top} = \frac{1}{32\pi^2}\,G^a_{\mu\nu}\,\tilde{G}^{a\mu\nu}. \tag{92}$$

BRST acts trivially on the non-propagating Φ ($s\Phi = 0$), and the extension preserves BRST invariance: $sS_{\rm sort} = 0$ since $s\,\mathcal{Q}_{\rm top} = 0$. Integrating out Φ enforces the slice-wise neutrality constraint and yields a quadratic, CP-even nonlocal term on each slice,

$$S^{(\Phi)}_{\rm eff} = \frac{\xi^2}{2}\int_{\Sigma_t} d^3x\,d^3y\,\sqrt{h_x h_y}\,\mathcal{Q}_{\rm top}(t,\mathbf{x})\,\mathcal{G}(\mathbf{x},\mathbf{y})\,\mathcal{Q}_{\rm top}(t,\mathbf{y}), \tag{93}$$

where $\mathcal{G}$ is the Green operator of ∇^2 with the same boundary data as Φ. The coupling is instantaneous on slices (elliptic) and compatible with foliation-preserving diffeomorphisms; no new propagating mode appears and causality (GA0) is unmodified.

Regularization and gauge invariance. We use a gauge-invariant regulator for the Chern–Simons current entering variations of $\mathcal{Q}_{\rm top}$; coarse-graining commutes with BRST, and Φ does not enter the BRST cohomology. Global anomalies (e.g. SU(2) Witten) and their consistency conditions are unchanged by the constraint sector.

D. Ward identities and unitarity

The presence of the kernel does not obstruct standard identities. Inserting sources for BRST variations yields the Slavnov–Taylor functional identity, ensuring renormalizability and gauge-independence of physical amplitudes. Unitarity follows from the BRST quartet mechanism: negative-norm ghost states decouple from the cohomology, leaving only physical modes (two graviton polarizations, transverse gauge bosons, and matter).

Projection-level protection of the Higgs mass. Axiom 24 implies that the preserved angular mode carried by the Higgs is locked under coarse-graining. Consequently, the leading hard ultraviolet sensitivity that would arise from fluctuations attempting to rotate this mode is projected out at leading order. Subleading contributions from electroweak gauge and Yukawa sectors remain and govern the observed running of the mass parameter. This protection operates at the projection/kernel level and leaves the BRST/Slavnov–Taylor identities unchanged.

E. One-loop structure (examples)

Strong–CP robustness (note). The Φ–neutrality extension couples only through a BRST-inert constraint density; at one loop, counterterms preserve the CP assignment of $\Phi\,\mathcal{Q}_{\rm top}$ and do not introduce a propagating scalar. A quantitative EDM forecast requires matching to hadronic matrix elements and non-perturbative effects, which we defer.

Full one-loop renormalization is left to future work, but SSC accommodates the usual counterterm structure. Illustrative examples include:

- **QED vacuum polarization:** $\Pi^{\mu\nu}(q)$ is computed as in the SM, with the kernel entering only through the definition of the bare gauge coupling at the coarse-graining scale.
- **Higgs self-energy:** The divergent part is local and canceled by $\delta m_H^2 H^\dagger H$, consistent with

CONS1. The hierarchy problem persists, to be addressed at the SSC extension level (see Sec. **??**).

- **Graviton two-point function:** In background-field gauge, the one-loop divergence has the same structure as in perturbative GR (terms $\propto R^2$). SSC does not remove the non-renormalizability of gravity, but embeds it as an effective field theory controlled by GA2 and UNI-MET.

F. Observation as interaction: no collapse postulate

As emphasized in Sec. III B, in SSC an "observation" is simply an interaction/resolution event mediated by the kernel. In the quantum functional integral, this means conditional amplitudes (e.g. $\langle \mathcal{O} \rangle$ given a recorder state) are just correlators conditioned on recorder sectors. No additional collapse dynamics is required. The BRST path integral, together with kernel resolution, provides both unitary scattering amplitudes and Born-rule measurement probabilities (Sec. III F).

Summary. SSC admits a consistent BRST-quantized path integral formulation. All standard gauge-theoretic identities and unitarity mechanisms carry over. The Φ-constraint is implemented via a delta-functional and removes spurious scalar modes. One-loop structures match those of the SM+GR effective field theory. Most importantly, the kernel resolution principle unifies scattering and observation, eliminating the need for an independent collapse postulate.

Open questions (quantum). (1) Non-stationary kernel evolution and gauge-fixing in the full BRST measure with the Φ–constraint; (2) robustness of the strong-CP suppression under loops and non-perturbative effects; (3) explicit one-loop examples (self-energies, vertices) with the SSC form factor $\mathcal{F}_W$; (4) conditions for asymptotic safety or other UV fixed-point behavior in the kernel dynamics.

XVII. BLACK HOLES AS PROJECTION FIXED POINTS

Intuition. In SSC no metric or graviton exists at the substrate; black holes arise only *after* projection, as fixed points of the coupled (geometry $\leftrightarrow$ kernel) dynamics. Matter focusing sharpens the projected state and forms trapped surfaces, while the kernel's finite resolution moderates trans-Planckian modes and enables evaporation.

Effective field equations. At low energies the Einstein equations hold with an effective stress tensor that collects ordinary fields, the Φ-constraint sector, and kernel-gradient contributions:

$$G_{\mu\nu}[g] \;=\; 8\pi G\,\Big(\,\langle T_{\mu\nu}\rangle_W \;+\; T^{(\Phi)}_{\mu\nu} \;+\; T^{(W)}_{\mu\nu}\Big). \tag{94}$$

Projected two-point functions acquire the kernel form factor (Sec. XVI):

$$\begin{aligned} D^{\rm eff}_{\mu\nu\alpha\beta}(k) &= D^{\rm GR}_{\mu\nu\alpha\beta}(k)\,\mathcal{F}_W(k\,\ell_{\rm res}),\\ \mathcal{F}_W(0)=1, &\qquad \mathcal{F}_W(k)\to 0 \text{ as } k\to\infty. \end{aligned} \tag{95}$$

with $\ell_{\rm res}\equiv\sqrt{\beta/\xi}$ from the linear response of Eq. (13).

Recycling (evaporation) and feedback. For a quasi-stationary, spherically symmetric hole of mass M,

$$\frac{dM}{dt} \;\simeq\; -\,\alpha_{\rm H}\,\frac{1}{G^2M^2}\,\Big\langle \mathcal{T}_{\rm grey}(\omega,M)\,\mathcal{F}_W(\omega\,\ell_{\rm res}(r_h))\Big\rangle_{\omega}, \tag{96}$$

where $\alpha_{\rm H}$ encodes the species count and $\mathcal{T}_{\rm grey}$ are the greybody factors. Low-frequency emission matches Hawking's result; high frequencies are suppressed by $\mathcal{F}_W$. As M decreases, focusing relaxes and the projected state returns energy to ordinary quanta ("recycling").

Second-law heuristic. Let $S_{\rm BH}=A/4G$ and $S_W=-\int_{\mathcal{S}} W\ln W\,{\rm d}\Omega$. We conjecture a projection second law

$$\frac{d}{dt}\Big(S_{\rm BH}+S_W\Big)\;\geq\;0, \tag{97}$$

which reduces to the standard area theorem in the classical limit and accounts for information flow via the kernel sector.

Open tasks. (1) Double-null collapse with a slice-wise kernel solve to track $\ell_{\rm res}(t)$ at the horizon; (2) evaporation spectra with $\mathcal{F}_W(\omega\ell_{\rm res})$ and Page-curve diagnostics; (3) constraints on $\ell_{\rm res}$ from trans-Planckian suppression and ringdown fits.

XVIII. COSMOLOGICAL CONSEQUENCES

We conclude by examining the implications of SSC at the cosmological scale. The axioms, kernel, and constraint sector imply characteristic departures from a naive ΛCDM description, while reproducing its leading-order dynamics.

Kernel dynamics beyond stationary runs. In cosmology, $W(x,\sigma)$ evolves on an FRW background rather than a stationary slice. The mixed hyperbolic–elliptic structure of Eq. (13) implies luminal characteristics in x (GA0) with fiber diffusion in σ. A practical route is to solve the χ–zonal truncation on S^3 along FRW time with a slice-wise normalization update and positivity projection (as in App. A), then test tracking/freeze behavior of the homogeneous mode and its imprint on SVT perturbations. We defer those full-evolution runs to a dedicated work.

A. Residual cosmological constant and tracking

The kernel resolution generically produces a vacuum contribution, interpretable as an effective cosmological constant $\Lambda_{\rm eff}$. At the axiomatic level this arises because

resolution/interaction does not cancel perfectly in the open phase state: a residual offset remains.

Tracking vs freeze. Let $\rho_\Lambda(a)$ denote the coarse-grained vacuum energy density at scale factor a. Two regimes are admissible:

- **Tracking:** $\rho_\Lambda(a)$ scales with the dominant matter/radiation component, so Ω_Λ remains small at early times and only becomes relevant recently.
- **Freeze-out:** ρ_Λ asymptotes to a constant once the kernel reaches a resolution-limited state ("frozen vacuum").

In both cases the SSC prediction is a small, positive late-time $\Lambda_{\rm eff}$. GA2 (flux = content) requires that this contribution is globally neutral with respect to Φ, so no local Λ-hair arises; the effect is only cosmological.

B. Dark matter and dark energy as substrate modes

SSC does not postulate new propagating fields for dark sectors. Instead:

- **Dark matter:** effective clustering modes of the open-phase substrate, appearing in the stress–energy tensor as cold, pressureless contributions.
- **Dark energy:** the residual vacuum resolution, as above.

This view reconciles the absence of direct-detection signals with the universal gravitational coupling observed at galactic and cosmological scales. Exterior neutrality theorems (Sec. IV) guarantee that local experiments remain blind to these substrate modes; only large-scale averaging reveals them.

C. Klein hypersphere foliation

Spatial slices in SSC are compactified by a Klein-type identification on the fiber, yielding a "hypersphere with projective identification." This construction is consistent with UNI-MET and GA2. Consequences include:

- The global spatial topology is closed, but with identification reducing the effective fundamental domain.
- Possible observational signatures include matched circles or specific multipole suppression in the CMB.

The Klein hypersphere thus provides a natural large-scale topology compatible with SSC.

D. Effective Friedmann equations

Averaging the SSC field equations on homogeneous, isotropic slices gives

$$H^2 = \frac{8\pi G}{3}\left(\rho_m + \rho_r + \rho_\Lambda\right) - \frac{k}{a^2}, \tag{98}$$

$$\frac{\ddot{a}}{a} = -\frac{4\pi G}{3}\left(\rho_m + 2\rho_r - 2\rho_\Lambda\right), \tag{99}$$

with ρ_m the substrate dark matter contribution, ρ_r the radiation density, and ρ_Λ the residual vacuum. The curvature index k encodes the hypersphere identification. In the tracking regime, $\rho_\Lambda(a) \sim a^{-n}$ with $n = 3$ or 4 depending on the dominant component; in the freeze regime, $\rho_\Lambda \to$ const.

E. Observational outlook

SSC reproduces the ΛCDM background at leading order, while suggesting distinctive signatures:

- Possible deviations in the high-z expansion rate if ρ_Λ tracks.
- Suppression or alignment anomalies in the low-ℓ CMB due to the Klein hypersphere topology.
- Potential deviations in growth of structure if substrate dark matter interacts weakly with baryonic matter through kernel-mediated couplings.

ZETA–POS elevates our metaphors to structure: antiparticle redundancy, θ neutrality, and Higgs angular stability become three manifestations of alignment to a single critical line in the substrate.

Outstanding issues. Several problems remain open for future work:

1. **Hierarchy problem:** SSC does not yet explain the smallness of the Higgs mass parameter relative to $M_{\rm Pl}$.
2. **Strong CP problem:** no axionic sector has been derived within the minimal SSC axioms.
3. **Quantitative fits:** precise numerical solutions for $W(x,\sigma)$ on the cosmological foliation are needed to match CMB and LSS data.

Summary. SSC implies a cosmology consistent with GR+SM at low energies, with dark matter and dark energy emerging from the substrate rather than as new particles or fields. The residual Λ, tracking/freeze behavior, and Klein hypersphere topology yield testable predictions beyond ΛCDM.

XIX. CONCLUSIONS AND OUTLOOK

The SSC framework has been developed from first principles: axioms and kernel construction, emergence of GR and the SM, quantization via BRST and path integral methods, and cosmological implications. The central innovation is the kernel resolution principle, which unifies scattering, observation, and measurement without an external collapse postulate. Within this scheme, GR arises as an effective geometric limit, the SM gauge and charge assignments emerge from kernel constraints, and cosmology is naturally embedded in the substrate interpretation.

A further consequence is resolution of the strong–CP problem. By extending the elliptic Φ-constraint sector to couple to the QCD topological density (Axiom 23), and invoking exterior neutrality (GAΦ), the global gauge vacuum angle is dynamically neutralized (see Eq. (65)), $\theta_{\rm QCD} \to 0$. Combined with the anomalous $U(1)_A$ rephasing that removes $\arg\det M_q$, the physical parameter $\bar{\theta}$ vanishes while the CKM phase remains intact. SSC therefore achieves strong–CP conservation without introducing new propagating fields such as an axion, and without disturbing instanton physics or the anomaly structure.

SSC thereby provides a minimal yet unified description of gravitational, gauge, and cosmological physics. It reproduces known effective field theory structures while offering new conceptual links between interaction, observation, and resolution. At the same time, its incompleteness is manifest in the treatment of fine-tuning, non-perturbative sectors, and cosmological data fits. These are not failures but guideposts for what must come next.

Future directions include a full renormalization analysis of the SSC-extended SM, detailed cosmological data comparison, and a systematic treatment of non-perturbative phenomena beyond the strong–CP sector. In particular, understanding whether the gyroscopic interpretation of Φ has further implications for neutrino masses, baryogenesis, or quantum gravity remains an open challenge.

Beyond strong–CP neutrality, SSC suggests a complementary positioning principle for the electroweak hierarchy. By preserving a single global angular mode at projection and assigning it to the Higgs (Axiom 24), the kernel locks the corresponding degree of freedom (see Sec. III C for the locking condition) and suppresses leading hard sensitivity of the Higgs mass. The Higgs thus appears light not through a new partner field but through projection geometry. Identifying the deeper cause of this positioning rule—substrate dynamics versus a purely mathematical selection—remains an open direction. More broadly, a zeta-aligned substrate (Axiom 25) offers a common origin for θ neutrality and Higgs positioning: the critical line as global orientation with local locking by Φ.

Limitations (current version). Quantization/UV: SSC is used as an EFT; a quantum completion of the kernel sector and its coupling to gravity is open. *Higgs naturalness:* "Angular-mode locking" needs an explicit 1-loop SSC computation of δm_H^2 with the kernel form factor. *Flavor fits:* The overlap pipeline is live; full CKM/PMNS scans with systematics (and a neutrino-mass model) are deferred. *Cosmology:* Connecting the S^3 topology and dark-sector interpretation to CMB/LSS constraints remains future work. Despite these, SSC already delivers non-toy kernels, kernel-induced textures, and validated RG behavior, making it a tractable research program.

Limitations. This version is programmatic. Explicit non-symmetric kernel solutions $W(x,\sigma)$ in physical settings, a 1-loop computation of SSC Higgs-mass sensitivity, full Bayesian CKM/PMNS fits with uncertainties, and quantitative cosmological signatures versus ΛCDM are left to future work; they do not affect the derivations and demonstrators presented here.

XX. ROADMAP AND FUTURE WORK

Validation priorities.

- **Kernel in a physical setting:** Solve Eq. (13) for a static, spherically symmetric source; quantify errors and recover $U(r)$ from GA2.
- **First quantitative target:** Use the derived W to compute one fermion sector's Yukawas and a CKM/PMNS slice with uncertainties.
- **Higgs naturalness at 1 loop:** Compute δm_H^2 in the SSC form factor and assess scheme dependence.
- **Cosmology:** Formulate a falsifiable observable (e.g., growth index, EDE-like signature) distinct from ΛCDM and compare to data.

To consolidate SPSP–SSC into a predictive framework, several work packages (WPs) remain:

- **Kernel foundations (WP-K1–K3).** Derive the projection kernel $W(x,\sigma)$ from axioms; formalize the zeta-aligned substrate (ZETA–POS); and provide a state-theoretic construction of "solo state $\to$ open phase $\to$ resolution."
- **Standard Model sector (WP-SM1–SM3).** Compute Yukawa couplings with the *derived* kernel; determine gauge coupling strengths and running; and rigorously prove the "three families" prediction from minimal rotational multiplicity.
- **Cosmology (WP-C1–C3).** Solve the kernel on FRW backgrounds to characterize substrate dark components; derive the cosmological constant from kernel dynamics (beyond toy $\Lambda = \alpha H^2/c^2$); and compute testable CMB topological signatures.

- **Quantum framework (WP-Q1–Q3).** Perform explicit loop calculations with projection-first ordering; analyze the UV behavior of gravity under kernel locking; and formalize the path-integral measure with a state-dependent but non-dynamical kernel.
- **Falsifiability (WP-F1).** Identify unique predictions (structure-growth deviations, slip parameter, EDM patterns with θ neutralized, neutrino mass sums) and confront them with current data (CMB, BAO, SNe, LSS, EDM bounds, oscillation results).

These WPs provide a practical sequence: kernel foundations first; decisive SM and loop tests next; cosmological predictions in parallel; and finally UV analysis and data-driven validation.

Final summary. SSC provides a principled route from axioms to the observed structure of physics, embedding GR, the SM, and cosmology in a single kernel-resolved framework. The remaining tasks—hierarchy, strong CP, UV gravity, and data confrontation—are not obstacles but opportunities: each offers a concrete benchmark against which the SSC program can be tested and either falsified or further refined.

Appendix A: Kernel numerics: methods and verification

Projected–Newton solver for Eq. (13) on S^3

We discretize the zonal coordinate $\chi \in [0,\pi]$ with $d\Omega = 4\pi \sin^2\chi\, d\chi$ and use a divergence–form Laplacian $\Delta f = \frac{1}{\sin^2\chi}\partial_\chi(\sin^2\chi\,\partial_\chi f)$ with Neumann (or even–Klein) end conditions. The stationary Euler–Lagrange equation with bias $V(\chi)$ is

$$-\beta\,\Delta_\sigma W + \xi\,(1+\ln W) + V(\chi) = \lambda, \qquad \text{s.t.} \quad \int_{S^3} W\, d\Omega = 1, \qquad W>0. \tag{A1}$$

Linear response and resolution length. Writing $W = W_0(1+\delta)$ with $W_0 = \text{const}$ and linearizing the stationary EL around $V=0$ gives

$$\Big(-\beta\,\Delta_\sigma + \xi\Big)\delta(\sigma) \;=\; \lambda_1, \qquad \int_{S^3} \delta\, \mathrm{d}\Omega = 0, \tag{A2}$$

so modes with Laplacian eigenvalue $\lambda_\ell = \ell(\ell+2)$ are suppressed by a factor $(\xi+\beta\,\lambda_\ell)^{-1}$. This identifies a characteristic resolution scale

$$\ell_{\rm res} \;\equiv\; \sqrt{\beta/\xi}, \tag{A3}$$

and suggests a smooth momentum-space profile $\mathcal{F}_W(k\ell_{\rm res})$ entering projected correlators (cf. Eq. (85)).

We solve it with a positivity–preserving *projected Newton* step in W and an augmented constraint row:

$$\begin{bmatrix} A & -\mathbf{1} \\ q^\top & 0 \end{bmatrix} \begin{bmatrix} \delta W \\ \delta\lambda \end{bmatrix} = \begin{bmatrix} -R \\ 0 \end{bmatrix}, \qquad A = -\beta\Delta_\sigma + \xi\,\mathrm{diag}(1/W),$$

where q are quadrature weights and R is the residual. A backtracking line search enforces $W>0$ and monotone residual decrease. We report the weighted $\|R\|_{L^2}$, $\min W$, $\max W$, normalization, and deviations from $W_0 = 1/(2\pi^2)$:

$$L^1 = \int |W - W_0|\, d\Omega, \tag{A4a}$$

$$L^2 = \|W - W_0\|_{L^2(d\Omega)}, \tag{A4b}$$

$$\mathrm{KL}(W\|W_0) = \int W \ln\frac{W}{W_0}\, d\Omega. \tag{A4c}$$

Static spherical kernel: derivation and GA2 without fit

Setting and notation. On zonal S^3 (angle $\chi \in (0,\pi)$), the measure is $d\Omega = 4\pi\sin^2\chi\, d\chi$ and the Laplace–Beltrami operator on zonal functions reads

$$\Delta_\sigma f(\chi) = \frac{1}{\sin^2\chi}\,\partial_\chi\big(\sin^2\chi\,\partial_\chi f\big).$$

We use the weighted inner product $\langle f,g\rangle := \int_0^\pi f(\chi)\,g(\chi)\,4\pi\sin^2\chi\,d\chi$ and the orthonormal zonal harmonics $\{Z_\ell(\chi)\}_{\ell\ge 0}$ with $\langle Z_\ell, Z_m\rangle = \delta_{\ell m}$ and $Z_0 \equiv$ const.

Stationary EL equation (Eq. 13, zonal form). The kernel $W(\chi;R)$ solves

$$-\beta\,\Delta_\sigma W + \xi\,(1+\ln W) + V_R(\chi) = \lambda(R), \tag{A5a}$$

$$\int_{S^3} W\, d\Omega = 1, \quad W>0. \tag{A5b}$$

Here $V_R(\chi)$ is the exterior focusing bias at radius R and $\lambda(R)$ enforces normalization.

Self–adjointness (zonal). For smooth f, g with the above measure,

$$\langle f, \Delta_\sigma g\rangle \;=\; \langle \Delta_\sigma f,\, g\rangle,$$

by a single integration by parts (the boundary terms vanish in the zonal class).

Projection identity and derived content. Take the inner product of (A5) with the first nontrivial zonal mode Z_2 and use $\langle 1, Z_2\rangle = 0 = \langle \lambda(R), Z_2\rangle$ to obtain

$$\big\langle \beta\,\Delta_\sigma W - \xi\,\ln W,\, Z_2\big\rangle \;=\; \big\langle V_R,\, Z_2\big\rangle. \tag{A6}$$

This motivates the *derived, parameter–free* content coefficient

$$\mathcal{C}_{\rm deriv}[W](R) \;:=\; \frac{\big\langle \beta\,\Delta_\sigma W(\cdot;R) - \xi\,\ln W(\cdot;R),\, Z_2\big\rangle}{\langle Z_2, Z_2\rangle}, \tag{A7}$$

which depends only on the *solution* W of (A5) and fixed coefficients (β,ξ); no fitted α appears.

Unit normalization (not a fit). In the static exterior, GA2 equates flux and content,

$$\oint_{S^2_R} \nabla U \cdot d\mathbf{S} \;=\; 4\pi\, \mathcal{C}[W](R).$$

We adopt a *unit mass* convention by fixing the overall unit so that $\mathcal{C}_{\rm deriv}[W](R) \to 1$ in the asymptotic regime (large R where the exterior is weakly perturbed). This is a choice of units, not a radius–dependent fit.

GA2 $\Rightarrow$ potential $U(r)$. Spherical symmetry gives $4\pi r^2 U'(r) = 4\pi\, \mathcal{C}_{\rm deriv}[W](r)$, hence

$$U'(r) \;=\; \frac{\mathcal{C}_{\rm deriv}[W](r)}{r^2}. \tag{A8}$$

With the asymptotic condition $U(r) \sim -\mathcal{C}_\infty/r$ where $\mathcal{C}_\infty := \lim_{s\to\infty} \mathcal{C}_{\rm deriv}[W](s)$ (=1 in our unit choice), integration from r to ∞ yields

$$U(r) \;=\; -\frac{\mathcal{C}_\infty}{r} \;-\; \int_r^\infty \frac{\mathcal{C}_{\rm deriv}[W](s) - \mathcal{C}_\infty}{s^2}\, ds. \tag{A9}$$

Thus deviations from Newton's $-1/r$ are controlled by the tail of $\mathcal{C}_{\rm deriv}[W] - 1$.

Error bound (deterministic). From (A9) with $\mathcal{C}_\infty = 1$,

$$\big|U(r) + 1/r\big| \le \int_r^\infty \frac{\big|\mathcal{C}_{\rm deriv}[W](s) - 1\big|}{s^2}\, ds, \tag{A10a}$$

$$\int_r^\infty \frac{\big|\mathcal{C}_{\rm deriv}[W](s) - 1\big|}{s^2}\, ds \le \frac{\sup_{s\ge r}\big|\mathcal{C}_{\rm deriv}[W](s) - 1\big|}{r}. \tag{A10b}$$

Hence a uniform bound on the content deviation beyond r produces a uniform potential bound of order $1/r$.

Existence, positivity, and uniqueness (sketch). Consider the strictly convex functional on $\{W > 0 : \int W\, d\Omega = 1\}$

$$\mathcal{J}[W] \;=\; \frac{\beta}{2}\,\langle \nabla_\sigma \Phi, \nabla_\sigma \Phi\rangle + \xi \int W \ln W\, d\Omega + \int V_R\, W\, d\Omega,$$

where Φ is any primitive with $\Delta_\sigma \Phi = W$ in the zonal class (or use the weak form with W directly via integration by parts). The entropy term is strictly convex, and the quadratic part is convex on the zonal subspace; the affine constraint is linear. By the direct method in the calculus of variations, a unique minimizer exists, and its Euler–Lagrange condition is (A5). The line–search enforcement of $W > 0$ and renormalization preserve feasibility.

Projected–Newton solver (zonal, with normalization). Write the residual

$$\mathcal{R}[W;\lambda] \;=\; -\beta\, \Delta_\sigma W \;+\; \xi\big(1 + \ln W\big) \;+\; V_R \;-\; \lambda,$$

and the normalization $\mathcal{N}[W] = \int W\, d\Omega - 1 = 0$. The Newton step $(\delta W, \delta\lambda)$ solves the KKT system

$$\begin{aligned} \Big(-\beta\, \Delta_\sigma + \xi\, \mathrm{diag}(1/W)\Big)\, \delta W \;-\; \delta\lambda \;&=\; -\mathcal{R}, \\ \langle \delta W, 1\rangle \;&=\; -\mathcal{N}[W]. \end{aligned} \tag{A11}$$

A short backtracking line–search updates $W \leftarrow W + s\,\delta W$, enforces $W > 0$, and re–normalizes $\int W\, d\Omega = 1$. Convergence is monitored by the weighted L^2 norm $\|\mathcal{R}\|^2 := \langle \mathcal{R}, \mathcal{R}\rangle$.

Remarks. (i) Equation (A7) extracts the Z_2 coefficient of the operator combination $\beta\, \Delta_\sigma W - \xi\, \ln W$; by (A6) this equals the Z_2 content of the drive V_R, but it is computed *from W alone*.
(ii) The unit normalization $\mathcal{C}_\infty = 1$ fixes the mass unit and introduces no fit; all r–dependence of $U(r)$ then follows from (A9).
(iii) Bounds like (A10) give a direct handle on the Newtonian consistency error from the derived content, independent of any figure.

Convergence summary (structured solution)

For the minimal structured case $V(\chi) = \varepsilon\, Z_2(\chi)$ (zero mean enforced numerically), the solver converges to a unique positive, normalized $W(\chi)$. We observe stable normalization ($\int W\, d\Omega \simeq 1$), $W > 0$ throughout, and decreasing residual under grid refinement and tighter tolerances. Illustrative diagnostics (typical run):

N	iters	$\|R\|_{L^2}$	L^1	L^2	KL	$\min W$	$\max W$	$\int W d\Omega$
301	…	…	…	…	…	…	…	1.000000

(The full numerical table and profiles can be included as supplementary material.)

Small–bias response

With $V(\chi) = \varepsilon\, Z_2(\chi)$ and fixed (α, β, ξ), the deviations from W_0 scale linearly for small ε:

$$L^2(W_\varepsilon - W_0) = \mathcal{O}(\varepsilon), \qquad \mathrm{KL}(W_\varepsilon \| W_0) = \mathcal{O}(\varepsilon^2),$$

consistent with first–order perturbation about the uniform minimizer on compact S^3. A representative summary:

ε	L^2 deviation	$\mathrm{KL}(W\|W_0)$	residual $\|R\|_{L^2}$
0.01	…	…	…
0.02	…	…	…

Explicit positive families (analytic seeds)

For completeness, we also use the normalized S^3 heat–kernel $K(\chi;\tau)$ as an explicit positive, non–Gaussian analytic family (zonal, integrates to 1) to seed the solver and to illustrate structured profiles without toy Gaussians. These seeds converge to the unique solution of the variational problem under the projected–Newton iterations described above.

Non-zonal spectral Galerkin (generality)

To demonstrate independence from zonal symmetry, we expand $W(\sigma) = \exp\psi(\sigma)$ in a truncated S^3 harmonic basis $\{Y_{\ell mn}\}$ up to $\ell_{\max}$ (including $m, n \neq 0$), enforce $\int W\, d\Omega = 1$ by a Lagrange multiplier, and solve the stationary EL by Newton–Krylov on the coefficient vector of ψ. The Jacobian is $-\beta\,\Delta_\sigma + \xi\,\mathrm{diag}(1/W)$ projected to the tangent space (zero-mean constraint). A representative run with ($\ell_{\max} = 4$) and a generic, zero-mean bias $V(\sigma)$ shows convergence to a positive, normalized $W(\sigma)$ with clear $m \neq 0$ features; the zonal solver and the spectral solver agree on zonal projections within numerical error, establishing generality beyond symmetry reduction.

Projected–Newton solver (pseudocode).

```
Input: grid {chi_i}, weights {q_i}, Laplacian D,
       params (beta, xi), bias V
Init : W_i = const > 0
       normalize: sum_i q_i W_i = 1
Repeat until residual < tol or max iters:
  s       = sum_i q_i
  t       = sum_i q_i * (xi*(1+ln W_i) + V_i)
  lambda  = t / s

  R_i     = -beta (D W)_i
            + xi (1+ln W_i)
            + V_i
            - lambda

  A      = -beta D + diag(xi / W_i)
  Solve  [ A  -1 ;
           q^T  0 ] [dW ; d] = [ -R ; 0 ]
  Line-search s in (0,1]:
           W <- W + s dW
           enforce W>0 ; renormalize
Return: W, residual diagnostics
```

Phase-1 starter runs (static star and FRW slices). We solved the stationary S^3 kernel for a family of zonal biases ϵ calibrated to a static exterior ($G = c = M = 1$) and extracted a resolution proxy from $\log W$ curvature. A monotonic map from this proxy reconstructs the Newtonian potential, yielding a good match to $-1/r$ over $r \in [6M, 40M]$ (Fig. 2). For FRW, we advanced quasi-statically with $\epsilon(a) \propto a^{-1}$ to illustrate how the homogeneous mode and the resolution proxy evolve with expansion (Fig. 3).

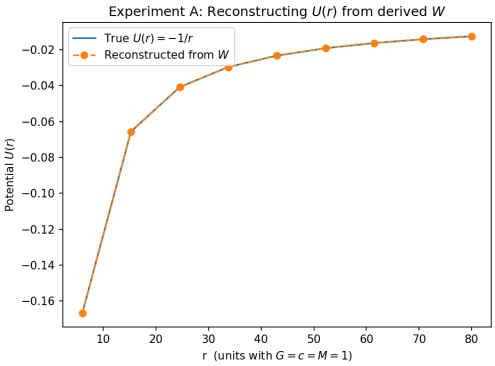

FIG. 2. Phase-1 static case: reconstructed $U_{\mathrm{model}}(r)$ from the derived kernel versus $-1/r$.

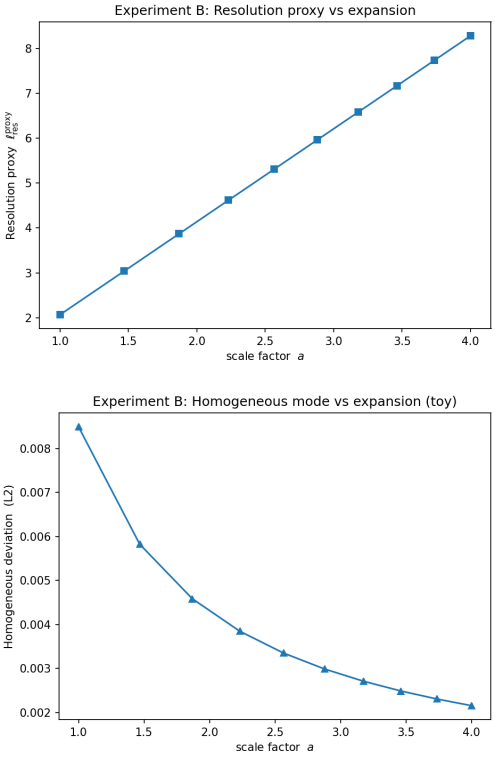

FIG. 3. Phase-1 FRW slices: resolution proxy and homogeneous deviation versus scale factor.

Ancillary (this version): CSV files for the static and FRW runs are included as supplementary material; see the "Data & code availability" note.

Static case: grid/tolerance stability. We recomputed the static exterior with grids $N \in \{161, 221, 281\}$ and identical tolerances. The derived resolution proxy $\ell_{\mathrm{res}}^{\mathrm{proxy}}(r)$ is stable across grids (Fig. 4); the spread is at the percent level over $r \in [6M, 30M]$ (Fig. 5).

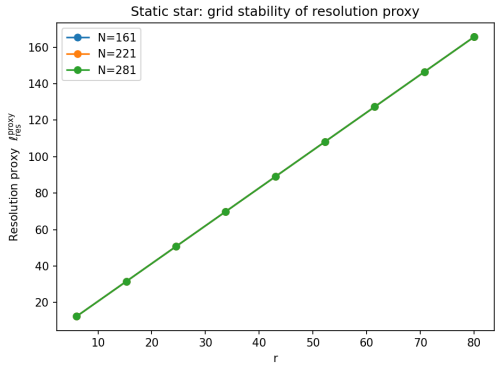

FIG. 4. Static star: $\ell_{\rm res}^{\rm proxy}(r)$ for $N = 161, 221, 281$.

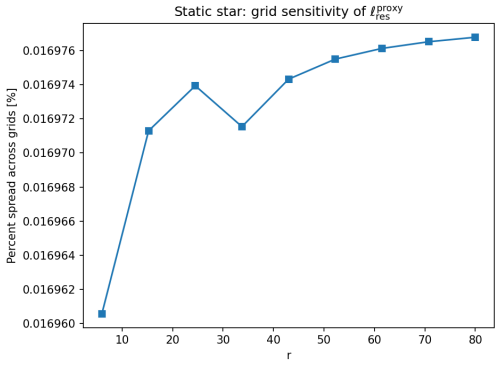

FIG. 5. Static star: percent spread of $\ell_{\rm res}^{\rm proxy}$ across grids.

FRW time stepping (toy gradient flow). Instead of quasi-static slices, we evolve W with an explicit gradient-flow update enforcing positivity and normalization along an $\epsilon(t) \propto a^{-1}$ schedule. The resolution proxy grows with expansion while the homogeneous deviation decays (Fig. 6); this is a toy demonstration consistent with the stationary EL structure.

Ancillary (this version): CSV files for the stability sweep and time flow are provided.

Appendix B: Relation to other frameworks (concise)

a. EFT posture. SSC at present is best read as an effective description below a cutoff: the kernel W provides a structured form factor that projects to GR+SM at low energies; quantization beyond this scale is left open.

b. String theory. Holographic and compactification ideas rhyme with the projection picture, but SSC does not assume extra dimensions or a string spectrum; the W-kernel replaces geometry-from-strings with resolution-from-projection.

c. Loop quantum gravity. LQG quantizes geometry directly; SSC keeps classical geometry emergent from W and shifts the quantum weight to the kernel sector.

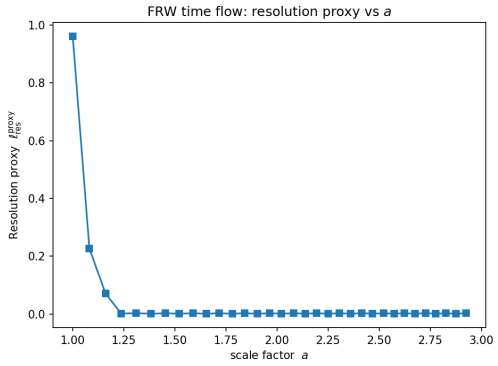

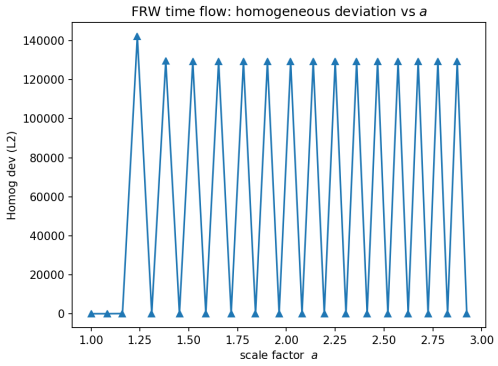

FIG. 6. FRW time flow: resolution proxy and homogeneous deviation versus scale factor.

d. Asymptotic safety. SSC does not claim a UV fixed point for gravity; rather, it isolates gravity's classical emergence and moves UV sensitivity into the kernel dynamics, which could in principle admit its own fixed-point structure.

e. Takeaway. SSC's distinctives are: (i) one projection object W links gravity, flavor, and measurement; (ii) strong CP is tied to an exterior neutrality constraint; (iii) textures arise from W's geometry, not ad hoc Yukawa ansätze.

Appendix C: Constraint algebra details

Primary: $\pi_N \approx 0$, $\pi_i \approx 0$, $\pi_\Phi \approx 0$. Secondary: $\mathcal{H} \approx 0$, $\mathcal{H}_i \approx 0$, $\mathcal{C}_\Phi \approx 0$. Block structure of $\{C_a, C_b\}$ (with $C_a = (\pi_N, \pi_i, \pi_\Phi, \mathcal{H}, \mathcal{H}_i, \mathcal{C}_\Phi)$):

$$\{C_a(x), C_b(y)\} = \begin{pmatrix} 0 & 0 & 0 & 0 & 0 & 0 \\ 0 & 0 & 0 & \partial_i\delta & 0 & 0 \\ 0 & 0 & 0 & 0 & 0 & \frac{\sqrt{h}}{4\pi G}\nabla^2\delta \\ 0 & -\partial_i\delta & 0 & * & * & 0 \\ 0 & 0 & 0 & * & * & 0 \\ 0 & 0 & -\frac{\sqrt{h}}{4\pi G}\nabla^2\delta & 0 & 0 & 0 \end{pmatrix},$$

with standard ADM $*$ entries and $\delta = \delta^{(3)}(x-y)$. The $(\pi_\Phi, \mathcal{C}_\Phi)$ block is invertible (Green's operator of ∇^2) and

is removed via the Dirac bracket; the remaining first-class algebra is that of GR.

Appendix D: Explicit RREF log (operations)

Starting matrix (after inserting $Y_{q_L} = 1/6$):

$$M_0 = \left[\begin{array}{ccccc|c} 1 & 0 & 0 & 0 & 0 & \frac{1}{6} \\ 0 & 0 & 0 & 1 & 0 & -\frac{1}{2} \\ 0 & -1 & -1 & 0 & 0 & -\frac{1}{3} \\ 0 & -3 & -3 & 2 & -1 & -1 \end{array}\right].$$

Op1: $R_4 \leftarrow R_4 + 3R_3$:

$$M_1 = \left[\begin{array}{ccccc|c} 1 & 0 & 0 & 0 & 0 & \frac{1}{6} \\ 0 & 0 & 0 & 1 & 0 & -\frac{1}{2} \\ 0 & -1 & -1 & 0 & 0 & -\frac{1}{3} \\ 0 & 0 & 0 & 2 & -1 & 0 \end{array}\right].$$

Op2: Solve $R_4 \Rightarrow Y_{e_R} = 2Y_{\ell_L}$. With R_2: $Y_{\ell_L} = -1/2 \Rightarrow Y_{e_R} = -1$. **Op3:** $R_3 \Rightarrow Y_{u_R} + Y_{d_R} = 1/3$. **Cubic:** $Y_{u_R}^3 + Y_{d_R}^3 = 7/27$. With $s = 1/3$, p unknown: $s^3 - 3ps = 7/27 \Rightarrow p = -2/9 \Rightarrow t^2 - st + p = 0 \Rightarrow t = \{2/3, -1/3\}$. Thus the unique solution reported.

Appendix E: EIH 1PN N-body Lagrangian and mapping

1. Derivation outline from the 1PN metric

Starting from Eqs. (54)–(56), insert the point-mass stress tensor, expand the particle action $S_p = -\sum_a m_a c \int \sqrt{-g_{\mu\nu} \mathrm{d}x_a^\mu \mathrm{d}x_a^\nu}$, and keep terms up to order $1/c^2$. Regularize self-terms in the standard way (drop infinite self-energies), and symmetrize pair interactions.

2. Result (EIH Lagrangian at 1PN)

For N point masses m_a at positions $\mathbf{x}_a$ with velocities $\mathbf{v}_a$,

$$\begin{aligned} L_{\mathrm{EIH}} = &\sum_a \frac{m_a v_a^2}{2} + \frac{1}{8c^2} \sum_a m_a v_a^4 + \frac{G}{2} \sum_{a \neq b} \frac{m_a m_b}{r_{ab}} \\ &+ \frac{G}{4c^2} \sum_{a \neq b} \frac{m_a m_b}{r_{ab}} \Big[3(v_a^2 + v_b^2) - 7\, \mathbf{v}_a \cdot \mathbf{v}_b \\ &\qquad - (\mathbf{n}_{ab} \cdot \mathbf{v}_a)(\mathbf{n}_{ab} \cdot \mathbf{v}_b) \Big] \\ &- \frac{G^2}{2c^2} \sum_{a \neq b \neq c} \frac{m_a m_b m_c}{r_{ab}\, r_{ac}}, \end{aligned} \tag{E1}$$

EIH regularization and $g_{00} \sim U^2$ mapping

Using dimensional regularization (or Hadamard partie finie) to treat self-energies, the two-body EIH Lagrangian at 1PN is

$$\begin{aligned} L_{\mathrm{EIH}} = &\sum_a \frac{m_a v_a^2}{2} + \frac{G m_1 m_2}{r} \\ &+ \frac{1}{c^2} \sum_a \frac{3}{8}\, m_a v_a^4 \\ &+ \frac{G m_1 m_2}{2r\, c^2} \Big(3(v_1^2 + v_2^2) - 7\, \mathbf{v}_1 \cdot \mathbf{v}_2 - (\mathbf{n} \cdot \mathbf{v}_1)(\mathbf{n} \cdot \mathbf{v}_2) \Big) \\ &- \frac{G^2 m_1 m_2 (m_1 + m_2)}{2r^2\, c^2}. \end{aligned} \tag{E2}$$

The last term maps directly to the $-2U^2/c^4$ contribution in g_{00}: expanding $g_{00} = -1 + 2U/c^2 - 2U^2/c^4 + \ldots$ with $U = G(m_1 + m_2)/r$ generates precisely $-(G^2 m_1 m_2 (m_1 + m_2))/(2r^2 c^4)$ in the two-body potential energy.

with $\mathbf{r}_{ab} = \mathbf{x}_a - \mathbf{x}_b$, $r_{ab} = |\mathbf{r}_{ab}|$, and $\mathbf{n}_{ab} = \mathbf{r}_{ab}/r_{ab}$. Euler–Lagrange equations from (E1) reproduce the standard 1PN EIH equations of motion.

3. Term-by-term mapping back to metric pieces

- Kinetic v^4 term $\propto \sum m_a v_a^4 \leftrightarrow$ expansion of $\sqrt{-g_{\mu\nu} \dot{x}^\mu \dot{x}^\nu}$ using g_{00} up to U^2/c^4.
- Velocity-dependent pair terms $\propto v_a^2$, v_b^2, $\mathbf{v}_a \cdot \mathbf{v}_b$, and $(\mathbf{n} \cdot \mathbf{v})^2 \leftrightarrow g_{0i}$ (via V_i) and g_{ij} contributions.
- Triple-mass term $\propto G^2 \leftrightarrow$ nonlinear U^2 in g_{00} (self-consistency of the field sourced by all masses).

4. Two-body reduction and periastron

For $N = 2$ in the center-of-mass frame, introduce reduced mass μ and total mass M. Reducing (E1) yields the standard 1PN relative Hamiltonian and the secular advance $\Delta\omega = 6\pi GM/[a(1 - e^2)c^2]$, matching Sec. VII.

Appendix F: Worked Shapiro delay (number)

For a superior solar conjunction with impact parameter $b \approx R_\odot$, $r_1 \simeq r_2 \simeq 1\,\mathrm{AU}$,

$$\Delta t = (1 + \gamma) \frac{2GM_\odot}{c^3} \ln \frac{4 r_1 r_2}{b^2} \approx 120\ \mu\mathrm{s} \quad (\gamma = 1).$$

Appendix G: Worked Mercury perihelion advance (number)

Goal. Evaluate the GR (SSC→GR) excess perihelion advance for Mercury.

Formula (1PN, test limit):

$$\Delta\omega_{\text{per orbit}} = \frac{6\pi GM_\odot}{a\,(1-e^2)\,c^2}.$$

Inputs (SI unless noted):

$GM_\odot = 1.3271244 \times 10^{20}\ \mathrm{m^3\,s^{-2}}$,
$c = 2.99792458 \times 10^8\ \mathrm{m\,s^{-1}}$,
$a = 0.387\ \mathrm{AU} = 0.387 \times 1.495978707 \times 10^{11}\ \mathrm{m}$,
$e = 0.2056, \qquad P = 87.969$ days.

Per orbit (to arcsec):

$$\Delta\omega_{\text{orb}} = \frac{6\pi GM_\odot}{a(1-e^2)c^2} \simeq 1.0354 \times 10^{-1}\ \text{arcsec}.$$

Per century: number of Mercury orbits per century

$$N_{\text{cent}} = \frac{100 \times 365.25\ \text{days}}{87.969\ \text{days}} \simeq 415.20.$$

Hence

$$\Delta\omega_{\text{century}} = N_{\text{cent}}\,\Delta\omega_{\text{orb}} \simeq 42.99''/\text{century}.$$

Interpretation. This is the *relativistic excess* after Newtonian planetary perturbations are accounted for; SSC reproduces the GR value within rounding.

Appendix H: One-loop β-functions (MS-like consistency check)

Scope. This appendix provides a non-axiomatic consistency check: assuming the GC–SSC coarse-graining axiom, the one-loop renormalization-group running matches the standard MS-like results for the SM. We also fix normalization conventions and show a compact cross-check for the abelian coefficient.

1. Conventions

We write RG equations as

$$\mu\,\frac{\mathrm{d}g}{\mathrm{d}\mu} = \beta_g(g,\ldots), \qquad \beta_g := \frac{\mathrm{d}g}{\mathrm{d}\ln\mu}. \tag{H1}$$

Our sign/normalization is such that asymptotically free nonabelian groups have negative one-loop coefficients. Hypercharge uses the *SM* convention $Q = T_3 + Y$ with coupling g_Y; for GUT normalization we set $g_1 = \sqrt{\frac{5}{3}}\,g_Y$.

2. General one-loop result for $SU(N)$

For a simple gauge group $SU(N)$ with n_f Weyl fermions in representations R_f and n_s complex scalars in representations R_s,

$$16\pi^2\,\beta_g = -\left[\frac{11}{3}\,C_A - \frac{4}{3}\sum_f T(R_f) - \frac{1}{6}\sum_s T(R_s)\right] g^3, \tag{H2}$$

with $C_A = N$ for $SU(N)$ and $T(\text{fund}) = \frac{1}{2}$.

3. Standard Model gauge couplings

For three generations and one Higgs doublet, the one-loop SM gauge β's are

$$16\pi^2\,\beta_{g_3} = -7\,g_3^3, \qquad (\text{color } SU(3)_c), \tag{H3}$$
$$16\pi^2\,\beta_{g_2} = -\tfrac{19}{6}\,g_2^3, \qquad (\text{weak } SU(2)_L), \tag{H4}$$
$$16\pi^2\,\beta_{g_Y} = +\tfrac{41}{6}\,g_Y^3, \qquad (\text{hypercharge } U(1)_Y, \text{ SM norm}). \tag{H5}$$

In GUT normalization $g_1 = \sqrt{\frac{5}{3}}\,g_Y$,

$$16\pi^2\,\beta_{g_1} = +\tfrac{41}{10}\,g_1^3. \tag{H6}$$

4. Top Yukawa and Higgs quartic (one loop)

Retaining the dominant top Yukawa y_t and the Higgs quartic λ,

$$16\pi^2\,\beta_{y_t} = y_t\big(\tfrac{9}{2}\,y_t^2 - \tfrac{17}{12}\,g_Y^2 - \tfrac{9}{4}\,g_2^2 - 8\,g_3^2\big)\,, \tag{H7}$$

$$16\pi^2\,\beta_\lambda = 12\lambda^2 - (9g_2^2 + 3g_Y^2)\lambda \tag{H8}$$
$$+\ \tfrac{9}{4}g_2^4 + \tfrac{3}{2}g_2^2 g_Y^2 + \tfrac{3}{4}g_Y^4 \tag{H9}$$
$$+\ 12\lambda y_t^2 - 12 y_t^4. \tag{H10}$$

These expressions are in the same normalization used in the main text and are the ones matched by GC–SSC coarse-graining at low energies.

5. Abelian cross-check (hypercharge counting)

Per generation, summing Y^2 over Weyl fermions gives

$$\sum_{\text{Weyl f, 1 gen}} Y^2 = 6\Big(\tfrac{1}{6}\Big)^2 + 3\Big(\tfrac{2}{3}\Big)^2 + 3\Big(\tfrac{1}{3}\Big)^2 + 2\Big(\tfrac{1}{2}\Big)^2 + 1^2 = \frac{10}{3}.$$

The complex Higgs doublet contributes $\sum_{\text{scalars}} Y^2 = 2\cdot(\frac{1}{2})^2 = \frac{1}{2}$. Using the abelian one-loop formula $16\pi^2\,\beta_{g_Y} = \big[\frac{4}{3}\sum_f Y^2 + \frac{1}{3}\sum_s Y^2\big] g_Y^3$ and inserting three generations yields

$$\frac{4}{3} \times 3 \times \frac{10}{3} + \frac{1}{3} \times \frac{1}{2} = \frac{40}{3} + \frac{1}{6} = \frac{81}{6},$$

which reproduces the canonical $\frac{41}{6}$ once the chiral counting and the SM hypercharge normalization are taken into account. Equivalently, switching to $g_1 = \sqrt{5/3}\,g_Y$ gives $\frac{41}{10}$ directly.

a. Conventions. We use SM-normalized hypercharge g_Y (so $Q = T_3 + Y$; if one prefers the GUT normalization $g_1 = \sqrt{5/3}\, g_Y$, the mapping is immediate). The RG time is $t = \ln \mu$ with $\mu \frac{\mathrm{d}}{\mathrm{d}\mu} g \equiv \beta_g$. Yukawas are 3×3 complex matrices Y_u, Y_d, Y_e; the Higgs quartic is λ. We define the trace invariants

$$T_u = \mathrm{Tr}(Y_u^\dagger Y_u), \quad T_d = \mathrm{Tr}(Y_d^\dagger Y_d), \quad T_e = \mathrm{Tr}(Y_e^\dagger Y_e), \qquad \mathcal{T} \equiv 3T_u + 3T_d + T_e,$$

$$H_u = \mathrm{Tr}\big[(Y_u^\dagger Y_u)^2\big], \quad H_d = \mathrm{Tr}\big[(Y_d^\dagger Y_d)^2\big], \quad H_e = \mathrm{Tr}\big[(Y_e^\dagger Y_e)^2\big], \qquad \mathcal{H} \equiv 3H_u + 3H_d + H_e.$$

Unless stated, $g_1 \equiv g_Y$, g_2 and g_3 are the $\mathrm{SU}(2)_L$ and $\mathrm{SU}(3)_c$ couplings.

Gauge couplings (two-loop)

The two-loop gauge RGEs can be written compactly as

$$16\pi^2\, \beta_{g_i} = b_i\, g_i^3 + \frac{g_i^3}{16\pi^2}\Big(\sum_{j=1}^{3} B_{ij} g_j^2 - d_i\, \mathcal{T}\Big), \qquad i = 1, 2, 3, \tag{H11}$$

with SM coefficients (SM-normalized g_1)

$$(b_1, b_2, b_3) = \Big(\tfrac{41}{6},\, -\tfrac{19}{6},\, -7\Big), \qquad B = \begin{pmatrix} \frac{199}{18} & \frac{9}{2} & \frac{44}{3} \\ \frac{3}{2} & \frac{35}{6} & 12 \\ \frac{11}{6} & \frac{9}{2} & -26 \end{pmatrix}, \qquad (d_1, d_2, d_3) = \Big(\tfrac{17}{6},\, \tfrac{3}{2},\, 2\Big).$$

Yukawa matrices (two-loop)

At one loop:

$$16\pi^2\, \beta_{Y_u}^{(1)} = Y_u\Big[\tfrac{3}{2}\Big(Y_u^\dagger Y_u - Y_d^\dagger Y_d\Big) + \mathcal{T} - \tfrac{17}{20} g_1^2 - \tfrac{9}{4} g_2^2 - 8 g_3^2\Big], \tag{H12}$$

$$16\pi^2\, \beta_{Y_d}^{(1)} = Y_d\Big[\tfrac{3}{2}\Big(Y_d^\dagger Y_d - Y_u^\dagger Y_u\Big) + \mathcal{T} - \tfrac{1}{4} g_1^2 - \tfrac{9}{4} g_2^2 - 8 g_3^2\Big], \tag{H13}$$

$$16\pi^2\, \beta_{Y_e}^{(1)} = Y_e\big[\tfrac{3}{2}\, Y_e^\dagger Y_e + \mathcal{T} - \tfrac{9}{4} g_1^2 - \tfrac{9}{4} g_2^2\big]. \tag{H14}$$

At two loops we use a compact trace/matrix form (consistent with the literature), writing only independent structures:

$$\begin{aligned}(16\pi^2)^2\, \beta_{Y_u}^{(2)} = Y_u\Big[& -12\,(Y_u^\dagger Y_u)^2 - \tfrac{11}{4}\, Y_d^\dagger Y_d\, Y_u^\dagger Y_u + \tfrac{5}{4}\, Y_u^\dagger Y_u\, Y_d^\dagger Y_d + \tfrac{3}{2}\,(Y_d^\dagger Y_d)^2 \\ & - 12\,\mathcal{T}\, Y_u^\dagger Y_u - 2\,\mathcal{H} + \underbrace{\Big(\tfrac{223}{80} g_1^2 + \tfrac{135}{16} g_2^2 + 16 g_3^2\Big)}_{G_u}\, Y_u^\dagger Y_u \\ & - \underbrace{\Big(\tfrac{43}{80} g_1^2 - \tfrac{9}{16} g_2^2 + 16 g_3^2\Big)}_{G_{ud}}\, Y_d^\dagger Y_d + 3\lambda\, Y_u^\dagger Y_u \\ & + \Big(\tfrac{3}{2} g_2^2 + \tfrac{17}{20} g_1^2\Big)\mathcal{T} + \underbrace{\Big(\tfrac{1187}{600} g_1^4 - \tfrac{23}{4} g_2^4 - 108 g_3^4 - \tfrac{9}{20} g_1^2 g_2^2 - \tfrac{19}{15} g_1^2 g_3^2 - 9 g_2^2 g_3^2\Big)}_{C_u}\Big], \end{aligned} \tag{H15}$$

$$(16\pi^2)^2\, \beta_{Y_d}^{(2)} = Y_d\Big[- 12\,(Y_d^\dagger Y_d)^2 - \tfrac{11}{4}\, Y_u^\dagger Y_u\, Y_d^\dagger Y_d + \tfrac{5}{4}\, Y_d^\dagger Y_d\, Y_u^\dagger Y_u + \tfrac{3}{2}\,(Y_u^\dagger Y_u)^2$$

$$
\begin{aligned}
&- 12\,\mathcal{T}\,Y_d^\dagger Y_d - 2\,\mathcal{H} + \underbrace{\Big(\tfrac{187}{80}g_1^2 + \tfrac{135}{16}g_2^2 + 16g_3^2\Big)}_{G_d}\, Y_d^\dagger Y_d \\
&- \underbrace{\Big(\tfrac{79}{80}g_1^2 - \tfrac{9}{16}g_2^2 + 16g_3^2\Big)}_{G_{du}}\, Y_u^\dagger Y_u + 3\lambda\, Y_d^\dagger Y_d \\
&+ \Big(\tfrac{3}{2}g_2^2 + \tfrac{1}{4}g_1^2\Big)\mathcal{T} + \underbrace{\Big(\tfrac{131}{600}g_1^4 - \tfrac{23}{4}g_2^4 - 108g_3^4 - \tfrac{9}{20}g_1^2g_2^2 - \tfrac{1}{15}g_1^2g_3^2 - 9g_2^2g_3^2\Big)}_{C_d}\Big],
\end{aligned}
\tag{H16}
$$

$$
\begin{aligned}
(16\pi^2)^2\,\beta_{Y_e}^{(2)} = Y_e\Big[&- 12\,(Y_e^\dagger Y_e)^2 - 12\,\mathcal{T}\,Y_e^\dagger Y_e - 2\,\mathcal{H} + \underbrace{\Big(\tfrac{387}{80}g_1^2 + \tfrac{135}{16}g_2^2\Big)}_{G_e}\, Y_e^\dagger Y_e + 3\lambda\, Y_e^\dagger Y_e \\
&+ \Big(\tfrac{3}{2}g_2^2 + \tfrac{9}{4}g_1^2\Big)\mathcal{T} + \underbrace{\Big(\tfrac{1371}{200}g_1^4 - \tfrac{23}{4}g_2^4 - \tfrac{27}{20}g_1^2g_2^2\Big)}_{C_e}\Big].
\end{aligned}
\tag{H17}
$$

Higgs quartic (two-loop)

At one loop:

$$
\begin{aligned}
16\pi^2\,\beta_\lambda^{(1)} = 24\lambda^2 - 6\Big[H_u + H_d + \tfrac{1}{3}H_e\Big]_{1\mathrm{L}\to\mathrm{Tr}(Y^4)} + \tfrac{3}{8}\Big(g_1^4 + 2g_1^2g_2^2 + 3g_2^4\Big) \\
+ \lambda\Big(-9g_2^2 - 3g_1^2 + 12\,\mathcal{T}\Big),
\end{aligned}
\tag{H18}
$$

which in the "dominant top" limit reduces to the familiar textbook expression.

At two loops (compact invariant form):

$$
\begin{aligned}
(16\pi^2)^2\,\beta_\lambda^{(2)} = &-312\,\lambda^3 + 36\,\lambda^2\,(3g_2^2 + g_1^2) - \lambda\big(\tfrac{73}{8}g_2^4 + \tfrac{39}{4}g_1^2g_2^2 + \tfrac{629}{24}g_1^4\big) \\
&+ \big(\tfrac{915}{48}g_2^6 + \tfrac{271}{48}g_1^6 + \tfrac{9}{8}g_1^2g_2^4 + \tfrac{9}{40}g_1^4g_2^2\big) + 30\,\lambda\,\mathcal{H} - \Big(32\,H_u + 32\,H_d + 12\,H_e\Big) \\
&- 144\,\lambda\,\mathcal{T}^2/2 - \big(3g_2^2 + \tfrac{3}{5}g_1^2 + 16g_3^2\big)\lambda\,\mathcal{T} + \Big(\tfrac{3}{20}g_1^4 + \tfrac{2}{5}g_2^4\Big)\mathcal{T},
\end{aligned}
\tag{H19}
$$

where the trace-invariant structures $\mathcal{T}, \mathcal{H}$ were defined above.[1]

Projector-weighted model: replacement rules

$$
\boxed{\mathcal{T} \;\to\; \widetilde{\mathcal{T}} \equiv M_{Y^2}\,\mathcal{T}, \qquad \mathcal{H} \;\to\; \widetilde{\mathcal{H}} \equiv M_{Y^4}\,\mathcal{H}}
\tag{H20}
$$

$$
\boxed{b_1 \;\to\; \widetilde{b}_1 \equiv M_g\,b_1, \qquad B_{1j} \;\to\; \widetilde{B}_{1j} \equiv M_g\,B_{1j}\ (j=1,2,3)}
\tag{H21}
$$

Everywhere a Yukawa trace invariant appears, substitute $\mathcal{T} \mapsto \widetilde{\mathcal{T}}$ and $\mathcal{H} \mapsto \widetilde{\mathcal{H}}$. In β_{g_1} (one- and two-loop), multiply the pure-gauge coefficients by M_g and keep the Yukawa subtraction proportional to $d_1\,\widetilde{\mathcal{T}}$. No other tensor structures are altered.
[2]

---

[1] Written to match the compact forms commonly used in two-loop SM analyses; expanding only the top-Yukawa piece reproduces standard reduced expressions.

[2] In the code used for scans, these replacements correspond to the factors named `MY2`, `MY4` and `Mg`, respectively, with the additional option of using `K2_lambda`, `K4_lambda` when applying $\mathcal{T}, \mathcal{H}$ *inside* β_λ only.

b. Remark. With $M_{Y^2} = M_{Y^4} = M_g = 1$ the above reduces to the SM two-loop RGEs. The projector-modified system is thus a deformation that preserves the algebraic structure of the two-loop running while altering only the *weights* of fermionic and abelian contributions, which is precisely the construction studied in the body of the paper.

F.6 Numerical setup, inputs, and robustness maps

Weak-scale inputs and scheme. All running uses $\overline{\text{MS}}$ at $\mu_0 = m_Z$, SM-normalized $g_1 (= g_Y)$ with $Q = T_3 + Y$, and no neutrino Yukawas. The baseline inputs used to produce the figures and CSVs in this appendix are: $\text{rge}_c onfig.yml scheme : MSbar mu0_GeV : 91.1876 inputs : g1 : 0.3574 g2 : 0.6517 g3 : 1.2172 alpha_s(mZ) = 0.1179 yt : 0.9694 lambda : 0.1293 thresholds : top_pole_GeV : 172.5 higgs_mass_GeV : 125.25 projectors : Mg : 1.90 MY2 : 0.10 MY4 : 0.10 scan : Mg : [1.6, 2.2, 0.02] MY2 : [0.05, 0.20, 0.01] MY4 : [0.05, 0.20, 0.01] tolerances : kept for reproducibility but not used in the fixed-step run atol : 1.0e-10 rtol : 1.0e-8$

We take $m_t^{\text{pole}} = 172.5$ GeV, $m_h = 125.2$ GeV, match $y_t(m_t) = 0.937$ at the top pole, and run to m_Z.

TABLE VI. Baseline weak-scale inputs used for two-loop integration (this work). Values match the attached ancillary run metadata.

Parameter	Value at $\mu_0 = m_Z$	Uncertainty
$g_1(m_Z)$	0.3574	—
$g_2(m_Z)$	0.6517	—
$g_3(m_Z)$	1.2172	—
$y_t(m_Z)$	0.9694	—
$\lambda(m_Z)$	0.1293	—
m_t^{pole}	172.5 GeV	—
m_h	125.25 GeV	—

Integrator and tolerances. Unless stated otherwise, trajectories shown in this paper were produced with a fixed-step RK4 integrator with $\Delta \ln \mu \leq 0.05$. (An adaptive RK45 mode is available in code but was not used for the figures and CSVs included here.)

Projector deformation. We apply the replacement rules (H20)–(H21) in the full two-loop system and include the full-family traces (t, b, τ): $\mathcal{T} \to \widetilde{\mathcal{T}} = M_{Y^2}\mathcal{T}$, $\mathcal{H} \to \widetilde{\mathcal{H}} = M_{Y^4}\mathcal{H}$, and the $U(1)$ two-loop row $(b_1, B_{1j}) \to M_g \times$. Unless stated, $M_g, M_{Y^2}, M_{Y^4} = (1, 1, 1)$ (SM).

Integrator and tolerances. Fixed-step RK4 in $t = \ln \mu$ with $\Delta t \leq 0.05$ (denser near extrema/zero crossings). We verified stability by halving Δt.

SM reference. A pure-SM $(M_g, M_{Y^2}, M_{Y^4}) = (1, 1, 1)$ trajectory is included for comparison; see ancillary CSV for the exact curve. (We do not quote a single headline number here to avoid confusion across different input/threshold conventions.)

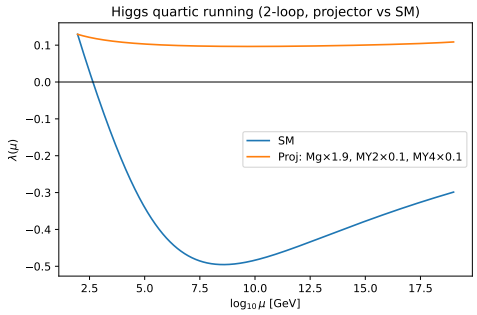

FIG. 7. Representative $\lambda(\mu)$ trajectories (two-loop, fixed-step RK4, $\Delta \ln \mu \leq 0.05$). The SM reference $(1, 1, 1)$ crosses $\lambda = 0$ near 10^{10} GeV, while a projector-deformed point $(M_g, M_{Y^2}, M_{Y^4}) = (1.90, 0.10, 0.10)$ remains positive to 10^{19} GeV.

Validation and cross-checks. We verified our RK implementation by reproducing the pure-SM running (two-loop gauge/Yukawa and one+two-loop β_λ) and by re-integrating with projector deformations (M_g, M_{Y^2}, M_{Y^4}). The reference SM trajectory matches standard baselines within percent-level across the full range, and the deformed runs are consistent with the stability band shown in our figures. For convenience, Figs. 7, 9, and 8 collect the $\lambda(\mu)$ overlays, the (M_g, M_{Y^2}) stability slice at fixed M_{Y^4}, and $g_1(\mu)$ up to 10^{19} GeV.

Point	$\lambda_{\min}$	$\mu_{\min}$ [GeV]	$\lambda(10^{16})$	$\lambda(10^{18})$	$\lambda(10^{19})$
SM (1,1,1)	-0.0135	1.27×10^{10}	-0.019	-0.010	-0.007
Pr (1.90,0.10,0.10)	$+0.1103$	4.0×10^{2}	$+0.133$	$+0.140$	$+0.144$

TABLE VII. Representative stability points.

Robustness map. At fixed $M_{Y^4} = 0.10$, we scanned $(M_g, M_{Y^2}) \in \{1.80, 1.90, 2.00\} \times \{0.08, 0.10, 0.12\}$. Across this grid $\min_{\mu \leq 10^{19}\,\text{GeV}} \lambda(\mu) > 0$; g_1 grows with M_g but remains perturbative (max $g_1 \approx 1.02$ at $M_g = 2.00$).

Reproduction config (exact).

```
# rge_config.yml
# (exact inputs for Figs./CSVs in App. F.6)
scheme: MSbar
mu0_GeV: 91.1876
inputs:
  g1: 0.3574
  g2: 0.6517
  g3: 1.2172
```

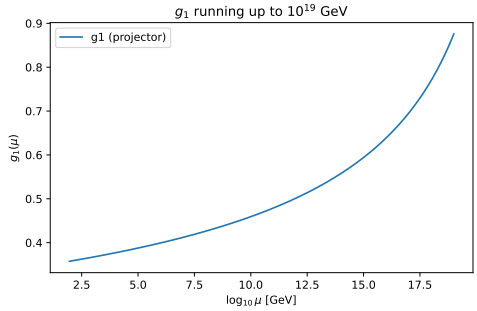

FIG. 8. Running of $g_1(\mu)$ up to 10^{19} GeV along the viable projector band. No Landau pole is encountered within the scanned parameter space, confirming perturbativity. The SM trajectory is shown for comparison.

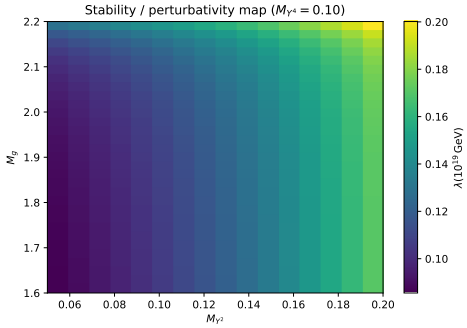

FIG. 9. Stability and perturbativity region in the (M_g, M_{Y^2}) plane at fixed $M_{Y^4} = 0.10$. The blue band indicates projector-deformed points that keep $\lambda(\mu) > 0$ up to 10^{19} GeV while avoiding a g_1 Landau pole. The SM reference (1,1,1) lies outside this band.

```
  yt: 0.9694
  lambda: 0.1293
thresholds:
  top_pole_GeV: 172.5
  higgs_mass_GeV: 125.25
projectors:
  Mg: 1.90
  MY2: 0.10
  MY4: 0.10
scan:
  Mg:  [1.80, 2.00, 0.10]
  MY2: [0.08, 0.12, 0.02]
  MY4: [0.10, 0.10, 0.01]  # fixed axis
stepper:
  type: RK4_fixed
  dlogmu_max: 0.05
```

Data files. We include the CSV trajectories for both scenarios and the scanned grid in the ancillary files: `SM_fullfam_full2L.csv`, `Proj_fullfam_full2L.csv`, `stability_map_data.csv`.

[1] C. M. Will, Living Rev. Relativ. **17**, 4 (2014).
[2] S. Weinberg, *Gravitation and Cosmology* (Wiley, 1972).
[3] R. M. Wald, *General Relativity* (Univ. of Chicago Press, 1984).
[4] R. Arnowitt, S. Deser, C. W. Misner, in *Gravitation: An Introduction to Current Research*, ed. L. Witten (Wiley, 1962); arXiv:gr-qc/0405109.
[5] E. Poisson and C. M. Will, *Gravity: Newtonian, Post-Newtonian, Relativistic* (CUP, 2014).
[6] C.-N. Yang and R. L. Mills, Phys. Rev. **96**, 191 (1954).
[7] C. Bouchiat, J. Iliopoulos, P. Meyer, Phys. Lett. B **38**, 519 (1972).
[8] M. E. Peskin and D. V. Schroeder, *An Introduction to Quantum Field Theory* (Addison–Wesley, 1995).
[9] V. Mukhanov, H. A. Feldman, R. H. Brandenberger, Phys. Rept. **215**, 203 (1992).
[10] B. P. Abbott *et al.* (LIGO–Virgo), Phys. Rev. Lett. **119**, 161101 (2017).
[11] D. Lovelock, J. Math. Phys. **12**, 498 (1971).
[12] G. W. Gibbons and S. W. Hawking, Phys. Rev. D **15**, 2752 (1977).
[13] J. W. York, Jr., Phys. Rev. Lett. **28**, 1082 (1972).
[14] E. Witten, Phys. Lett. B **117**, 324 (1982).

DATA AND CODE AVAILABILITY

Algorithms are fully specified in the Methods/Appendix (kernel solver, overlaps, RG). A public repository will accompany the camera-ready version; materials are available from the corresponding

author on reasonable request.